Development and Applications of Dense Optical Flow for New Generation Satellite Imagery

Presenting Author: *Jason Apke[1]*

With contributions from: *Steven Miller[1], Kris Bedka[2], Dan Lindsey[3], Kyle Hilburn[1], Matt Rogers[1], Chris Velden[4], Robert Rabin[5], and Thomas Vandal[6]*

[1] *Cooperative Institute for Research in the Atmosphere (CIRA), Fort Collins, CO*
[2] *NASA Langley Research Center, Hampton, Virginia*
[3] *NOAA Center for Satellite Applications and Research, Fort Collins, CO*
[4] *Cooperative Institute for Meteorological Satellite Studies (CIMSS), University of Wisconsin-Madison, Madison, WI*
[5] *NOAA/National Severe Storms Laboratory, Norman, OK*
[6] *NASA-Ames Research Center, Moffett Field, CA*

Introduction

Additional information can be extracted from satellite imagery if we take advantage of motions in fine-temporal resolution data!

Can you see the cyclonic rotation of Hurricane Michael?

At 15 & 10 min, all we can really see is translation of the eye

At 5 min, slower cyclonic motion is observed at the cloud-tops

At 1 min & 30 sec, the fast-moving eye wall motions are observable!

This number represents the image refresh rate

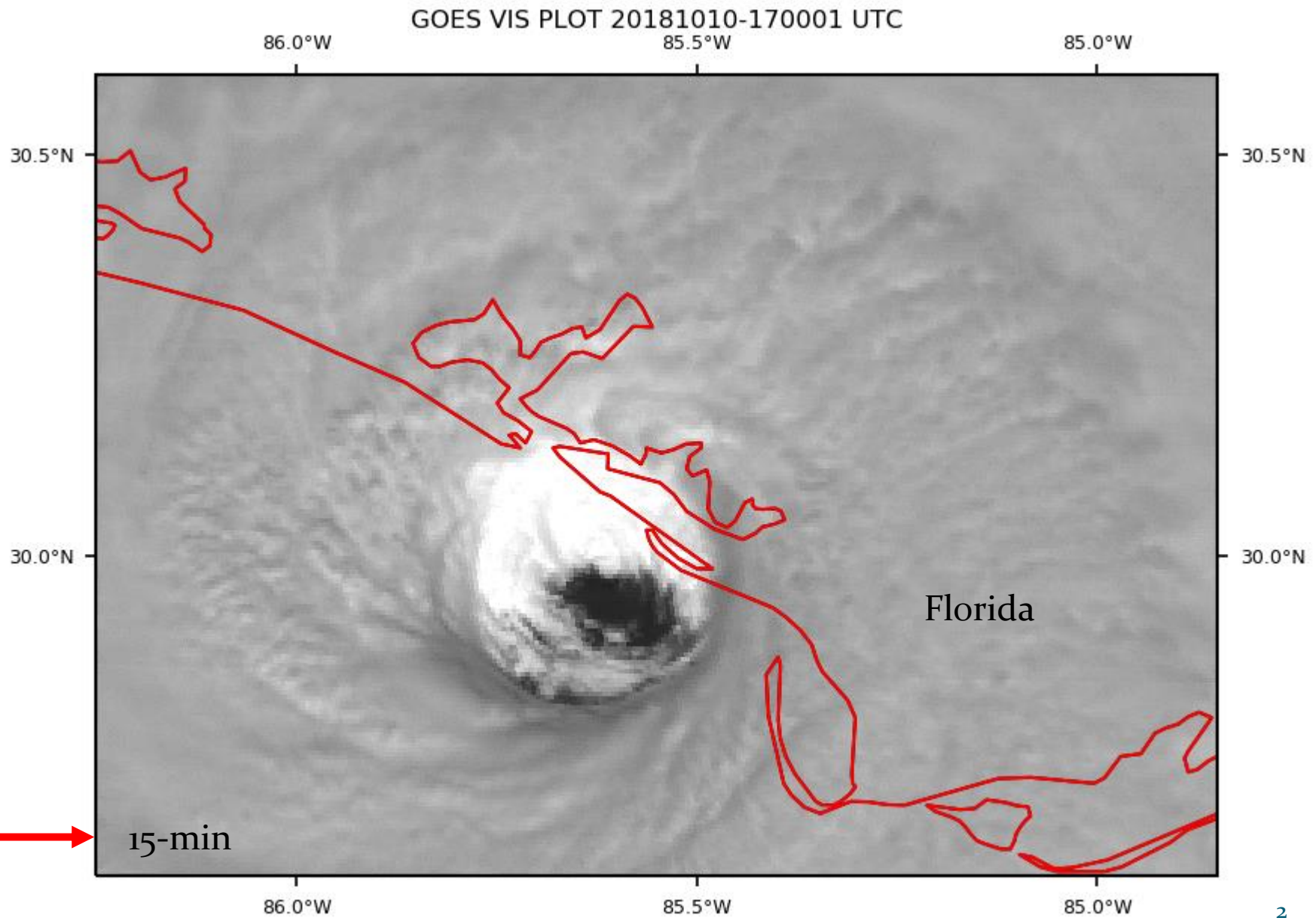

Introduction

- As satellite imagery improves, our subjective ability to identify motion improves, which should translate to improved objective identification
- Recent studies have found diagnosis and forecasting value in mesoscale-flow derived with passive high spatial, temporal, and spectral resolution satellite image sequences (Wu et al. 2016; Apke et al. 2016; 2018; Velden et al. 2017; Oyama et al. 2018; Otsuka et al. 2019; Stettner et al. 2019; Sandmæl et al. 2019; Apke et al. 2020; Mecikalski et al. 2020 *In Review.*)
- Many new and advanced so-called "optical flow" techniques for extracting more motion from image sequences have been developed, which we currently do not take advantage of!
- The goal of this ongoing work is to bring cutting edge optical flow derivation techniques and their benefits to satellite research and operations

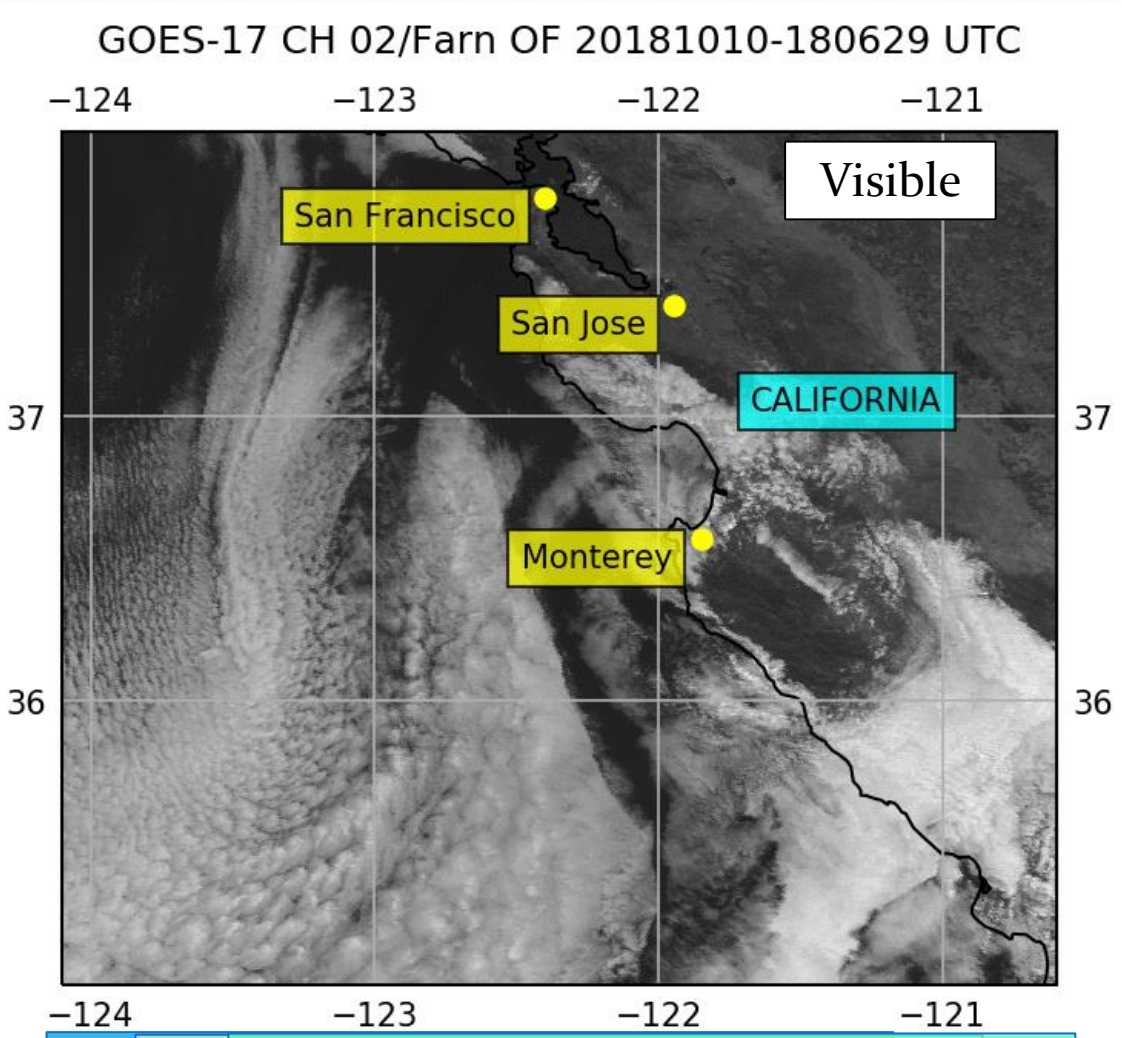

Op "Sp "Dense" Optical Flow Definition:

Motions are derived at EVERY image pixel the image are derived (e.g Derived Motion Winds; DMWs; Bresky et al. 2012)

Optical Flow Applications

- Applications OUTSIDE atmospheric sciences (to name a few):

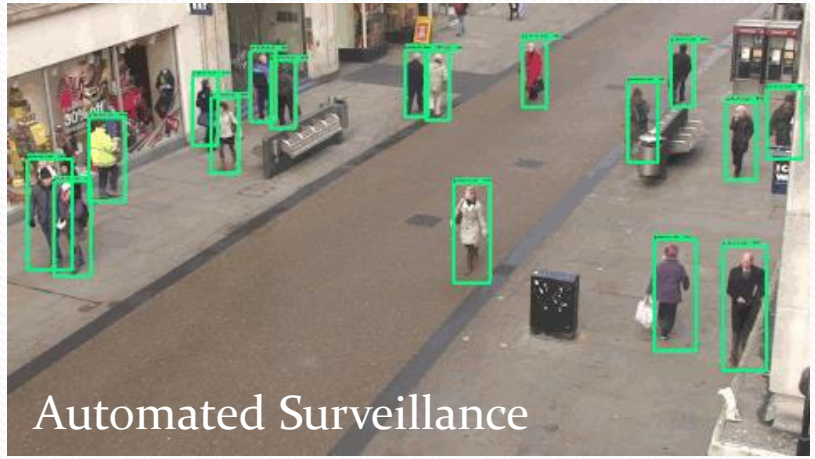

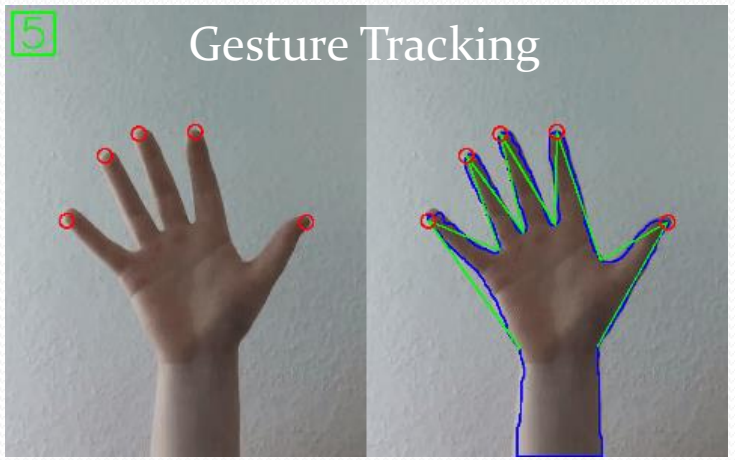

Sources (top left to bottom right): media.giphy.com, medium.com, androidpolice.com, Tao et al. (2012), metro.co.uk, gifs.com

Why Now?

- Assumptions within Dense Optical Flow derivation algorithms are better when displacements are small and natural cloud variability (from evaporation and condensation) between images is low (Fortun et al. 2015)
  - Targets are easier to track with shorter time-steps between images
- The Geostationary Operational Environmental Satellite (GOES)-R successfully launched in November, 2016, carries the Advanced Baseline Imager (Schmidt et al. 2017)
  - Spatial Resolution: Heritage: ~1 km visible Next Generation: ~500 m VIS, ~2 km IR
  - Spectral Resolution: Heritage: 1 VIS, 4 IR Channels, GOES-R: 2 VIS, 14 IR Channels
  - Radiometric Resolution: Heritage: 10 Bit Image, GOES-R 12 Bit
  - Temporal Resolution- Heritage: Up to 5 minute, GOES-R: Routine 1-min, up to 30 sec
- There are new geostationary satellites with similar capabilities to GOES-R coming online around the globe
  - Himawari AHI, Meteosat Third Generation FCI, FY-4A

Talk Outline

1) Derivation of Optical Flow
   - Background (and Current Techniques in Satellite Meteorology)
   - Assumptions Made
   - Methods for Computation
   - Strengths/Weaknesses of Current Approaches
   - Dense Optical Flow Derivation Techniques
2) Satellite Meteorology Applications of Optical Flow Algorithms
   - More Winds!
   - Inter-Frame Interpolation (Pseudo Super Rapid Scan Satellite Imagery)
   - Feature Tracking (BIG for machine learning projects)/Cloud-Top Cooling
   - Miscellaneous
3) Validation of Optical Flow
4) Additional work by the Mesoscale Winds Working Group

Brief Background

- In the 1960's, Ted Fujita's group were among the first to research gridding, navigation and quality control of satellite imagery required for cloud-drift wind derivation from satellite imagery
- In 1966, ATS-1 was launched, providing the first geostationary satellite images for weather analysis
  - "The clouds move – not the satellite." (Suomi 1969)
- In the 1970's, the first winds derivation systems emerged, and were automated over the next few decades(e.g. Schmetz et al. 1993; Velden et al. 1997; Bresky et al. 2012)

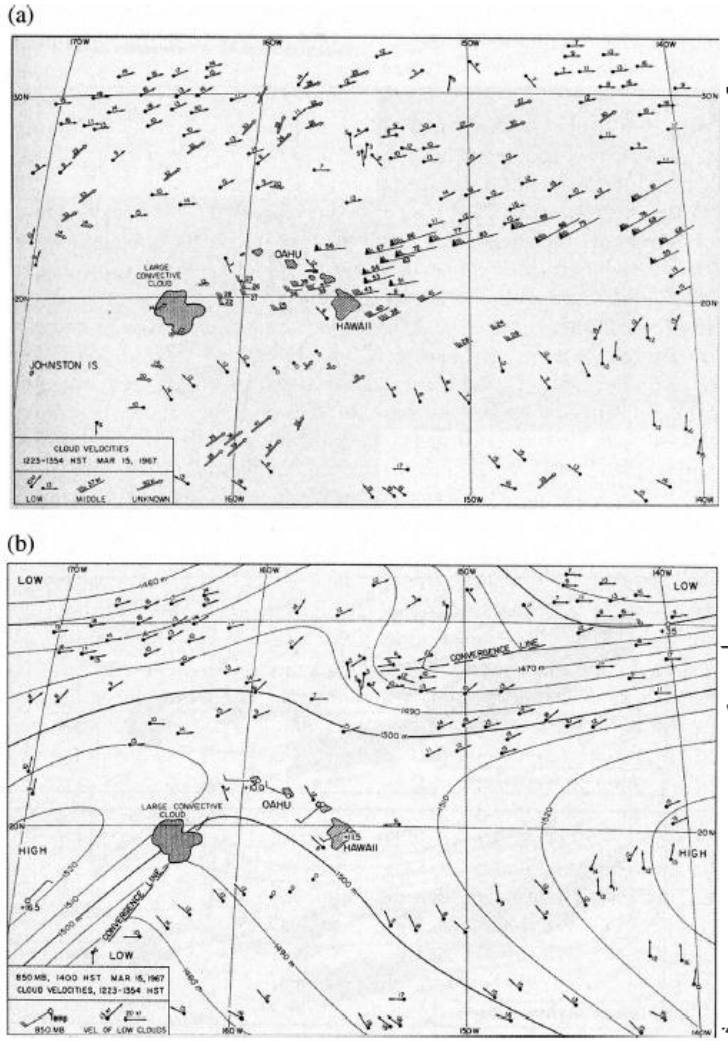

FIG. 3. (a) Computed velocities of cloud elements selected as good tracers. The velocities were computed from the cloud displacements during the period between 1223 and 1354 HST on 15 Mar 1967. (b) Low cloud velocities inferred from ATS images on 15 Mar 1967 superimposed on the 850-hPa analysis; the large convective cloud in the ATS image is clearly located on a convergence line.

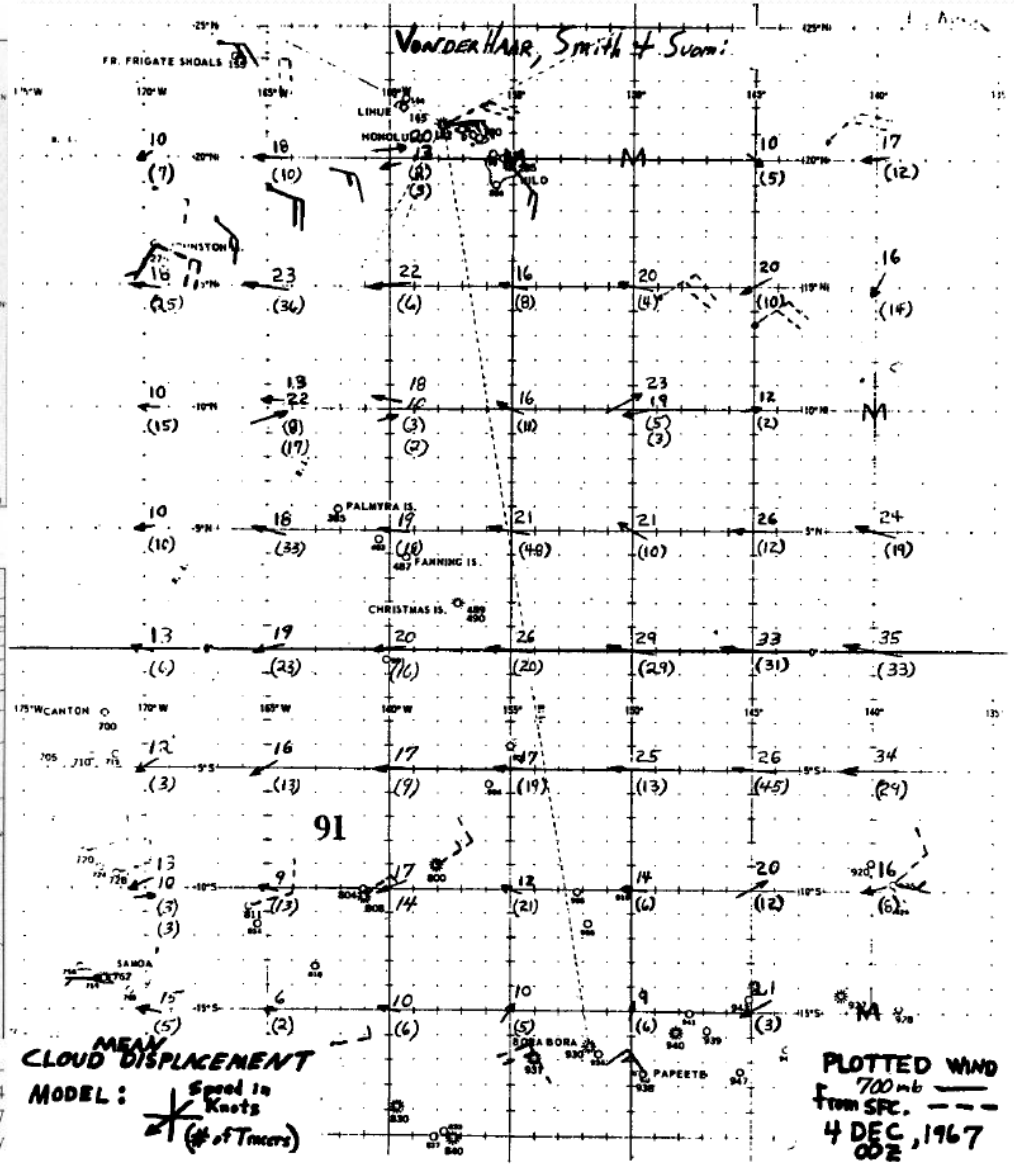

Fig. 8(b). Computer derived winds

Current Motion Derivation Methods

- DMWs (also called Atmospheric Motion Vectors) are derived from a sequence of (typically 3) GOES Images
- Step 1: Identify target in VIS/IR/WV Imagery
- Step 2: Height Assign target with IR and WV data in comparison to Numerical Weather Prediction (NWP) Fields (Nieman et al. 1993)
- Step 3: Forecast displacement and search for target in next image (minimize sum-of-square error), resulting displacement is the AMV (DMWs then cluster tracked results over a larger target area)
- Step 4: (Optional) Quality control with NWP and Neighboring AMVs for synoptic scale flow
- Important: These techniques struggle in image regions w/ motion discontinuities (i.e. transparent or multi-layer clouds), illumination changes, rotation/deformation, lack of texture

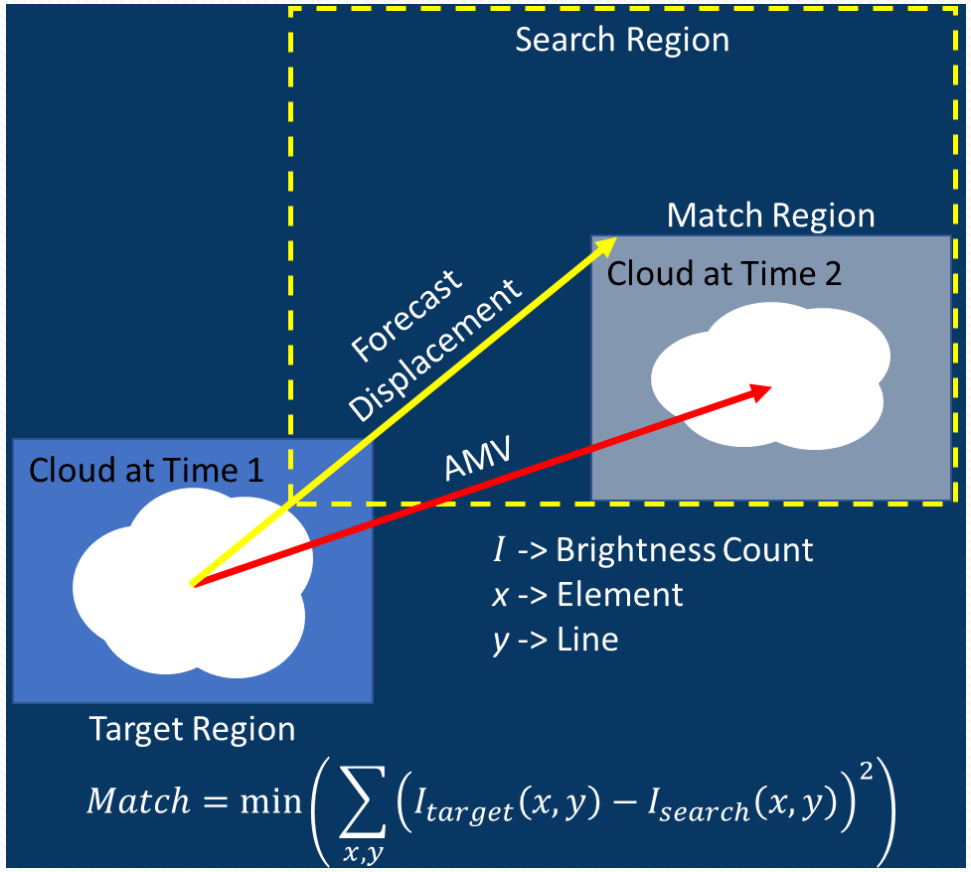

Figure 1. Schematic of AMV derivation concept using the Heritage feature tracking algorithm. For three images, this is performed twice, forwards (like that shown above) and backwards in time, and the two AMVs are averaged to produce a final motion estimate (Adapted from Bresky et al. 2012).

Current Motion Derivation Methods

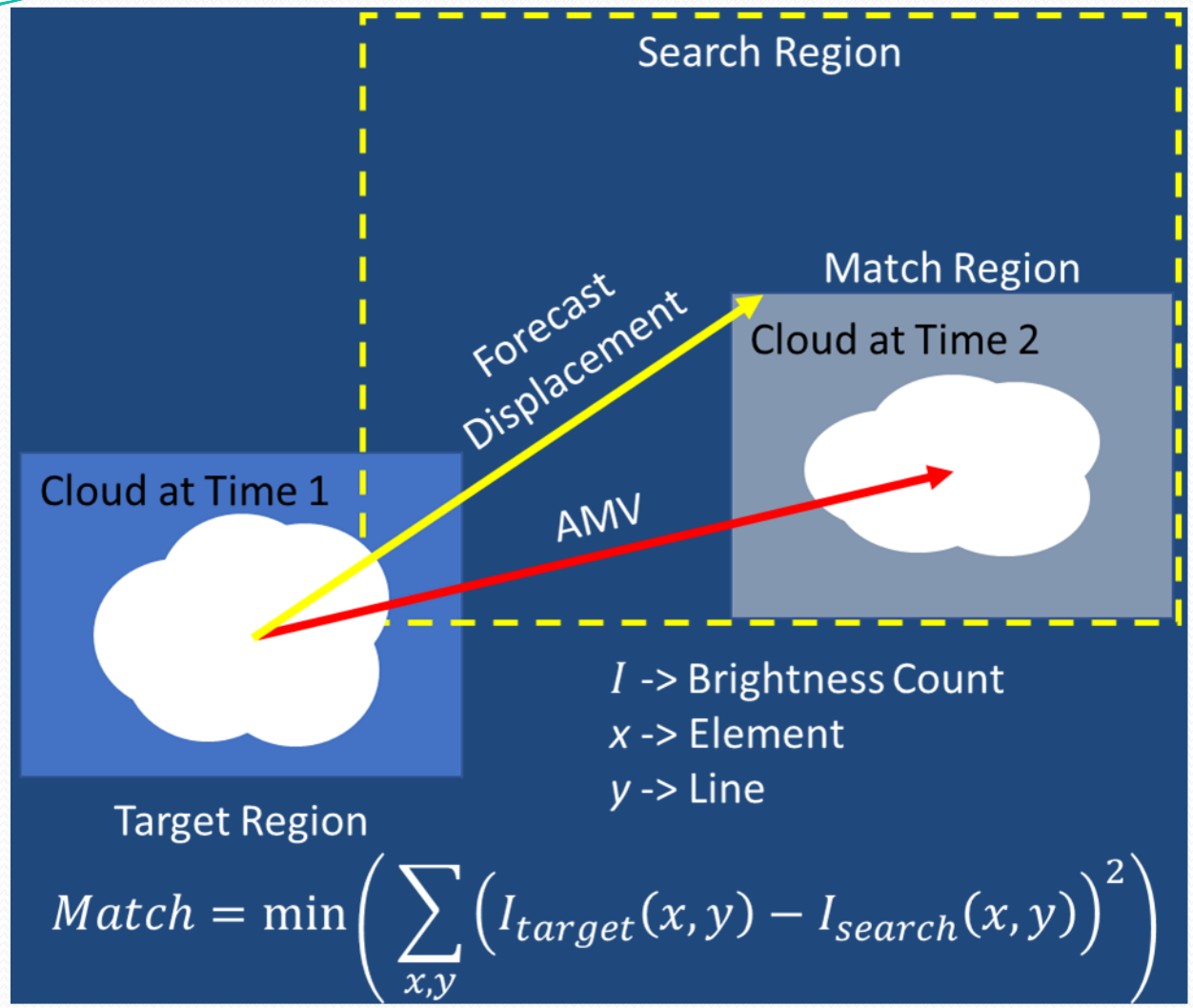

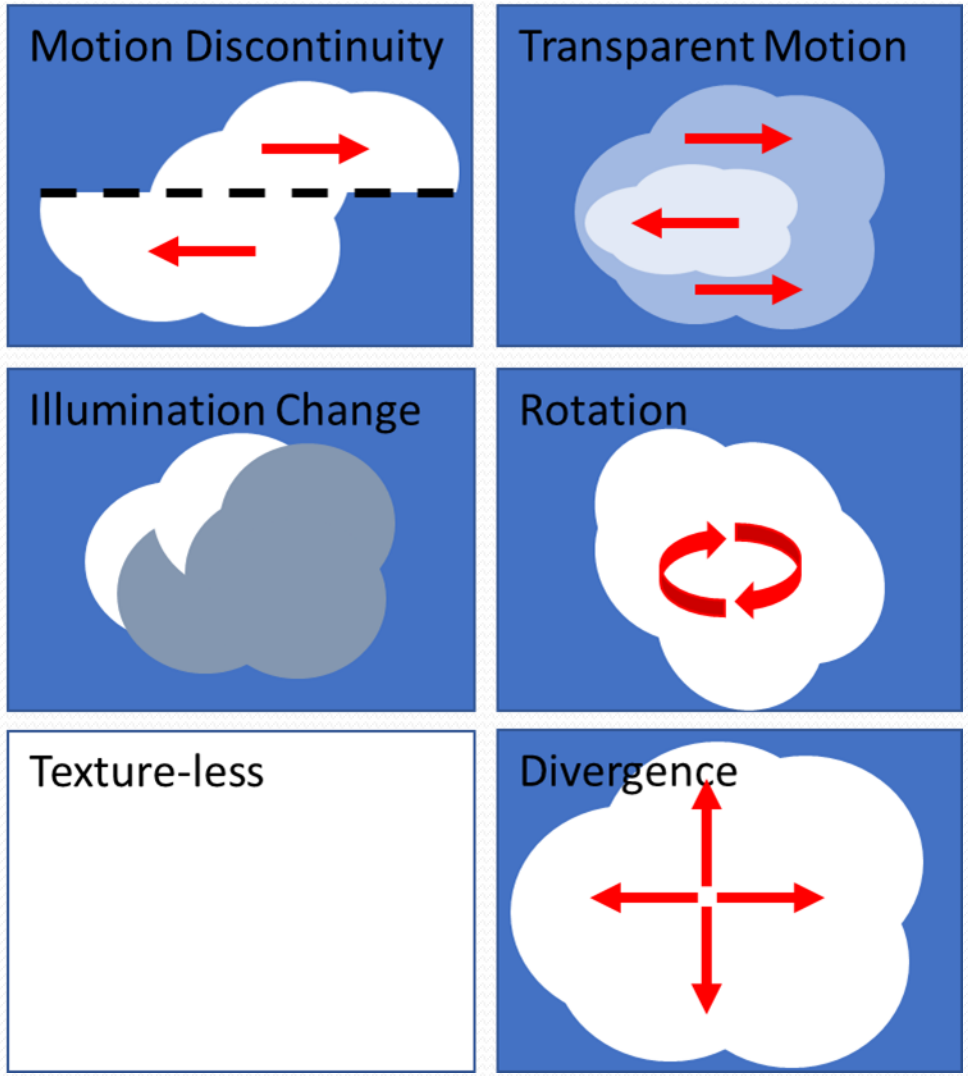

This approach fails if → Any one of these happen

Optical Flow Derivation Techniques

- Optical Flow Algorithms work by minimizing "energy" produced by violation of predetermined constraints
- Remember the AMV example? The <u>local</u> energy is:

$$E(u,v) = \sum_{x,y \in N_i} \left(I_{target}(x,y,t) - I_{search}(x+u, y+v, t+\Delta t) \right)^2, \text{ where } E(u,v) \rightarrow energy,$$

$$N_i \rightarrow Every\ pixel\ in\ the\ target\ region$$

- u and v are estimated by testing a valid search region for the minimum value of $E(x,y)$
  - In most operational algorithms that do this, energy is estimated for the surrounding pixels, and quadratic interpolation is performed to estimate the sub-pixel-based u, v
- The above assumes that brightness changes only as a function of motion u and v
  - *This assumption is called Brightness Constancy constraint*
  - It tends to fail when clouds condense or evaporate!
- When optical flow is derived using only pieces of the image, it is called a "Local" approach
  - Advantages: fast, you can identify which targets give you the best solutions, and it can retrieve large displacements
  - Disadvantages: Not computable everywhere!

Global Optical Flow Techniques

- Local techniques still breakdown without some other constraint when there is no texture
- Another approach is to minimize energy over the entire image called a "Global Technique"
- Horn and Schunck (1981), for example, minimize:

$$E(u(\boldsymbol{x}), v(\boldsymbol{x})) = \iint_{\Omega} |I(\boldsymbol{x} + \boldsymbol{U}, t + \Delta t) - I(\boldsymbol{x}, t)|^2 + \alpha\, SC\, d\boldsymbol{x}$$

$$\Omega \rightarrow Every\ pixel\ in\ the\ image$$

SC = Smoothness Constraint (or "regularizer") -> $|\nabla u|^2 + |\nabla v|^2$, α = constant weight of SC

- To solve the above, the brightness constancy constraint is linearized (subscripts are partial derivatives) …

$$I(\boldsymbol{x} + \boldsymbol{U}, t + \Delta t) - I(\boldsymbol{x}, t) \rightarrow I_x u + I_y v + I_t$$

- …and the Euler-Lagrange equations are used ($E(u(\boldsymbol{x}), v(\boldsymbol{x}))$ minimized when):

$$\frac{\partial E}{\partial u} - \frac{d}{dx}\left(\frac{\partial E}{\partial u_x}\right) - \frac{d}{dy}\left(\frac{\partial E}{\partial u_y}\right) = 0$$

$$\frac{\partial E}{\partial v} - \frac{d}{dx}\left(\frac{\partial E}{\partial v_x}\right) - \frac{d}{dy}\left(\frac{\partial E}{\partial v_y}\right) = 0$$

Global Optical Flow Techniques

- For Horn and Schunck (1981), that results in this sparse system of linear equations:

$$I_x^2 u + I_x I_y v - \alpha \nabla^2 u = -I_x I_t$$

$$I_x I_y u + I_y^2 v - \alpha \nabla^2 v = -I_y I_t$$

- We want the above in terms of

$$\boldsymbol{A}\,\vec{x} = \vec{b}$$

- The trick is that x -> all flow values in the image (see image)
- Horn and Schunck solve with Gauss-Seidel iterations (though there are now many sparse matrix solver libraries out there today)
- Note: there are limitations to linearizing brightness constancy!
- This (and local) methods do not yet account for motion discontinuities!

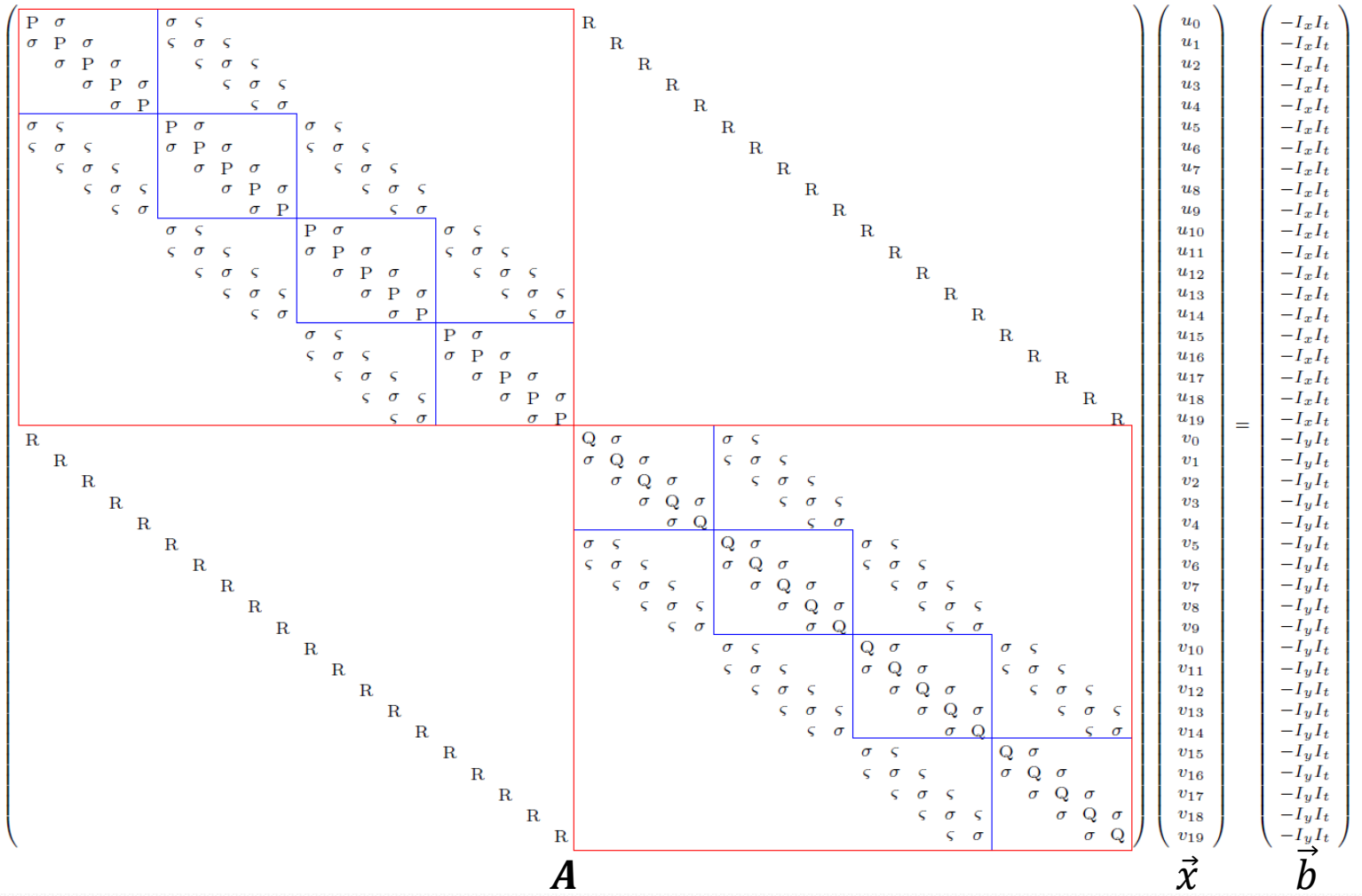

Source: Meinhardt-Llopis, E., J. Sánchez Pérez, and D. Kondermann, 2013: Horn-Schunck Optical Flow with a Multi-Scale Strategy. *Image Process. Line*, **3**, 151–172, doi:10.5201/ipol.2013.20.

Flow Linearization

- Most optical flow techniques depend on some sort of linearization of brightness and/or gradient constancy to minimize energy equations, e.g.

$$BC \rightarrow I(\boldsymbol{x} + \boldsymbol{U}, t + \Delta t) = I(\boldsymbol{x}, t) \approx$$

$$0 = I_x u + I_y v + I_t + \cancel{HOT}$$

$$subscripts \rightarrow deriviatives$$

- Linearization introduces problems, for example, let's assume:

$$0 = I_x u + I_t$$

This implies we can solve for $u = -I_t / I_x$

- When displacements are large and non-linear, most optical flow derivation methods fail!
- There are solutions to this problem…

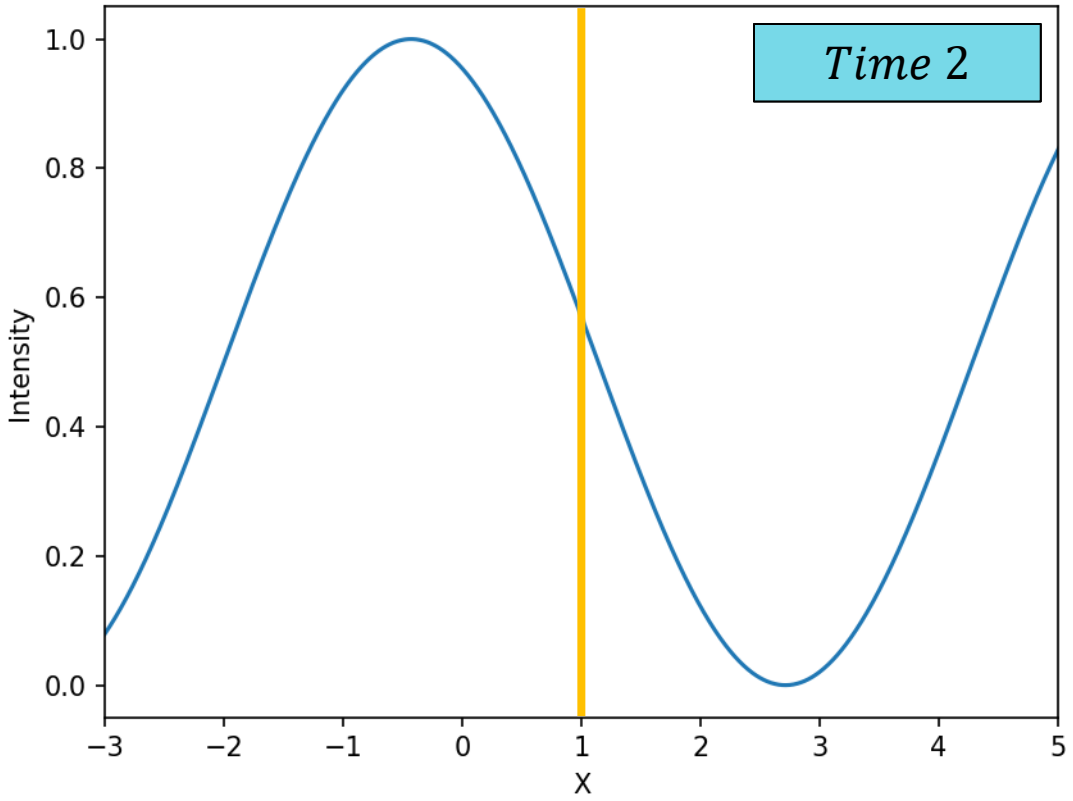

$I_x \approx 0.27$ $I_t \approx -0.35$
Estimated $u = 1.29$, Actual $u = -2$

Handling Large Displacements

- When displacements are large, many optical flow algorithms use a "Coarse-to-fine" technique to guess initial motion while keeping constraint linearization
- Step 1) Subsample image to a coarse enough resolution such that all motions are ~ < 1 pixel
- Step 2) Estimate optical flow at the coarsest resolution
- Step 3) Upscale optical flow estimated to next finest resolution, use it as initial guess to the motion
- Step 4) Repeat step 3 until you reach the native resolution
- Disadvantage: Coarse initial guesses will smooth out smaller (in space) motions!
- Next-generation satellites enable us to use dense optical flow methods with new rapid scanning rates!

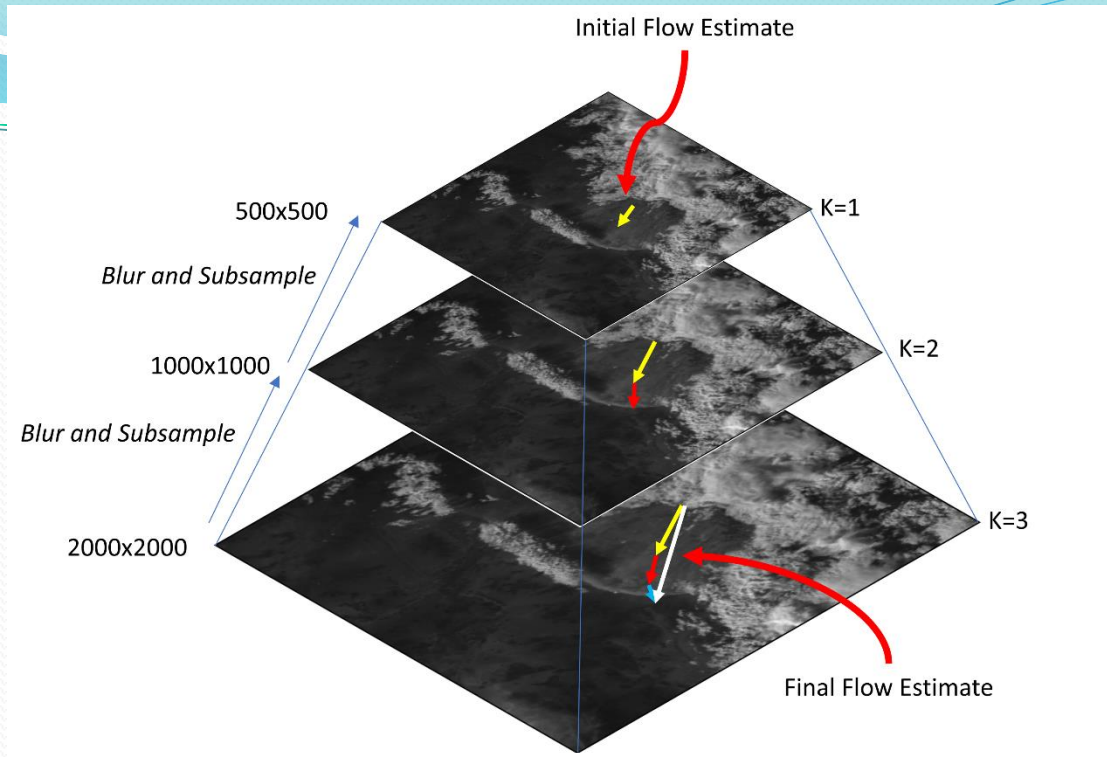

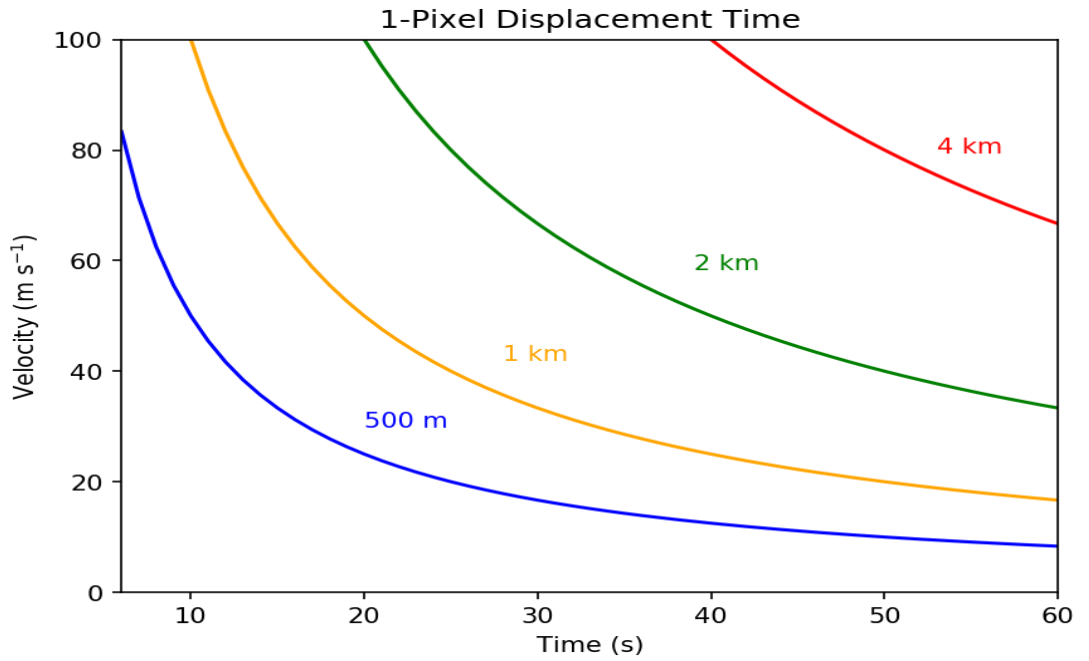

Network Design

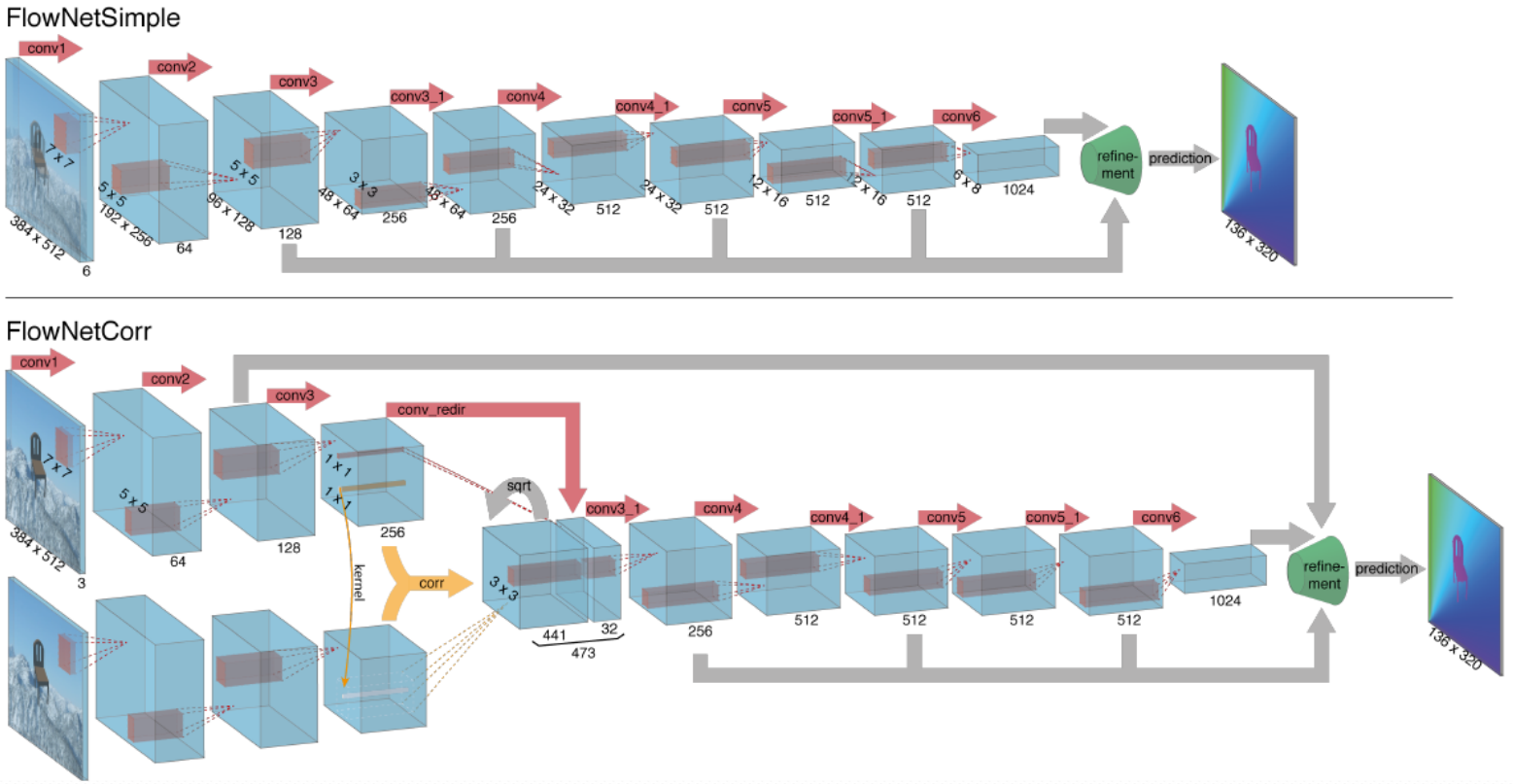

Synthetic Training Datasets

Testing Datasets

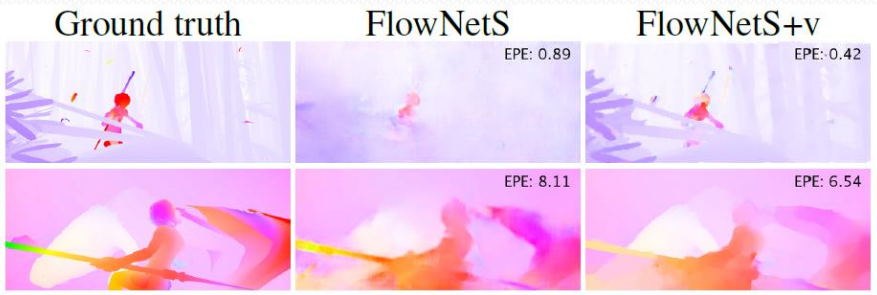

Source of Images: Fischer, P., and Coauthors, 2015: FlowNet: Learning optical flow with convolutional networks. *Proc. IEEE Int. Conf. Comput. Vis.*, **2015 Inter**, 2758–2766, doi:10.1109/ICCV.2015.316.

- Recent optical flow research resolves large displacements, as well as issues related to occlusions, image noise/blur using Machine Learning/Neural Network techniques
- Advantages: Can resolve motions for highly non-linear sequences, end models are very computationally efficient
- Disadvantages: Training datasets may not be representative of real motion, they can struggle at resolving small “outlier” motions, resolving why flows are incorrectly derived can be very difficult

Handling Motion Discontinuities

- For Horn and Schunck (1981) heavily penalizes the presence of motion discontinuities

$$E(u(\boldsymbol{x}), v(\boldsymbol{x})) = \iint_{\Omega} |I(\boldsymbol{x} + \boldsymbol{U}, t + \Delta t) - I(\boldsymbol{x}, t)|^2 + \alpha\, SC\, d\boldsymbol{x}$$

- Black and Anandan (1996) show that a simple change to the energy equation allows multiple layers to be preserved, so

$$E(u(\boldsymbol{x}), v(\boldsymbol{x})) = \iint_{\Omega} \rho_d(BC) + \alpha\, \rho_s(SC) d\boldsymbol{x}$$

- ρ_d and ρ_s are robust functions designed to soften the penalization of large outliers on the energy function, and are typically set to the Charbonnier penalty:

$$\rho_d(x^2) = \rho_s(x^2) = \sqrt{x^2 + \varepsilon^2},\ where\ \varepsilon^2 = 0.0001$$

- Black and Anandan's equation can be solved with the same Euler Lagrange equation minimization process, though typically the sparse matrix problem must be solved multiple times to account for nonlinearities associated with the robust functions
  - A good example: Brox, T., A. Bruhn, N. Papenberg, and J. Weickert, 2004: High accuracy optical flow estimation based on a theory for warping. 2004 *Eur. Conf. Comput. Vis.*, **4**, 25–36.

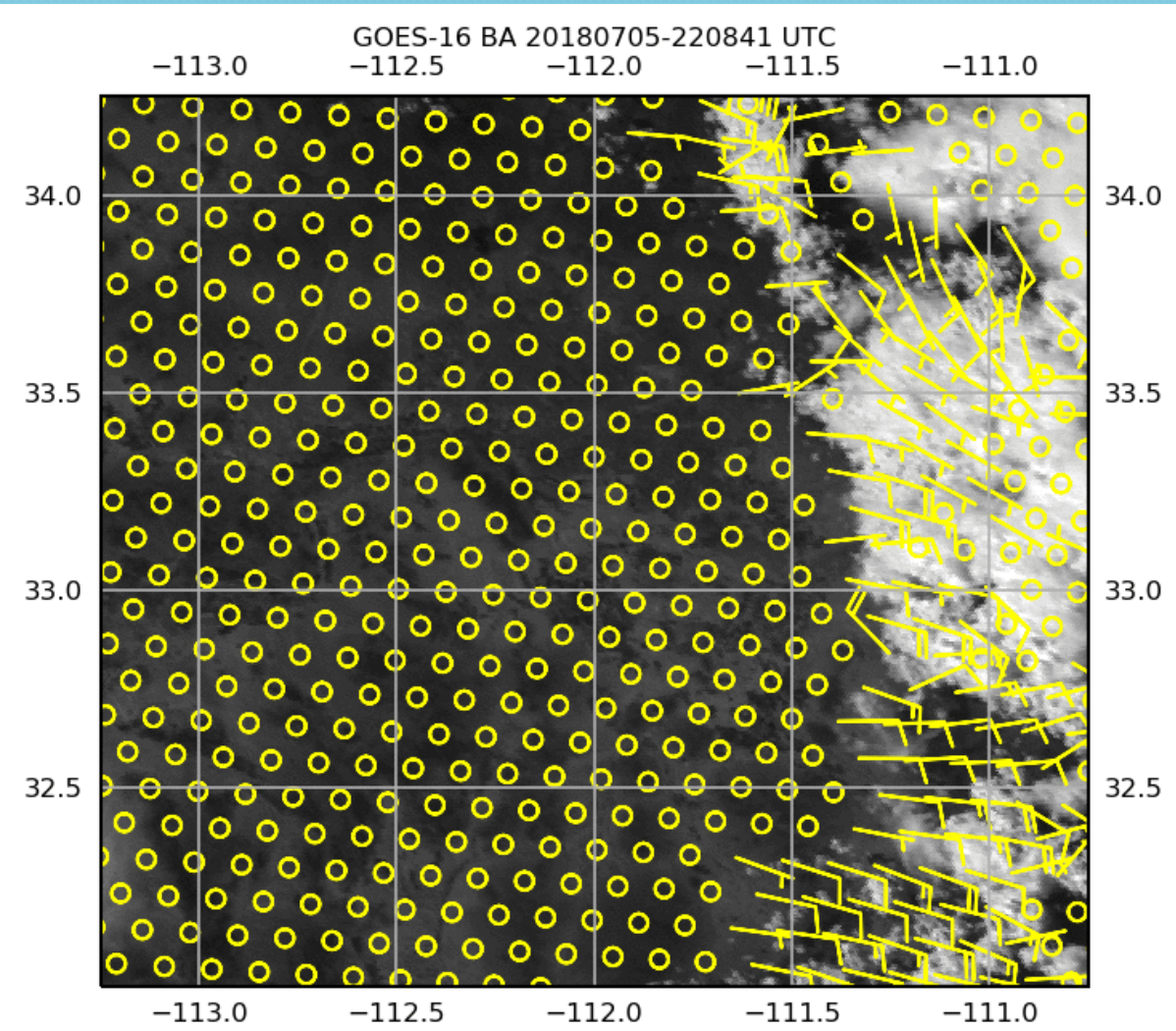

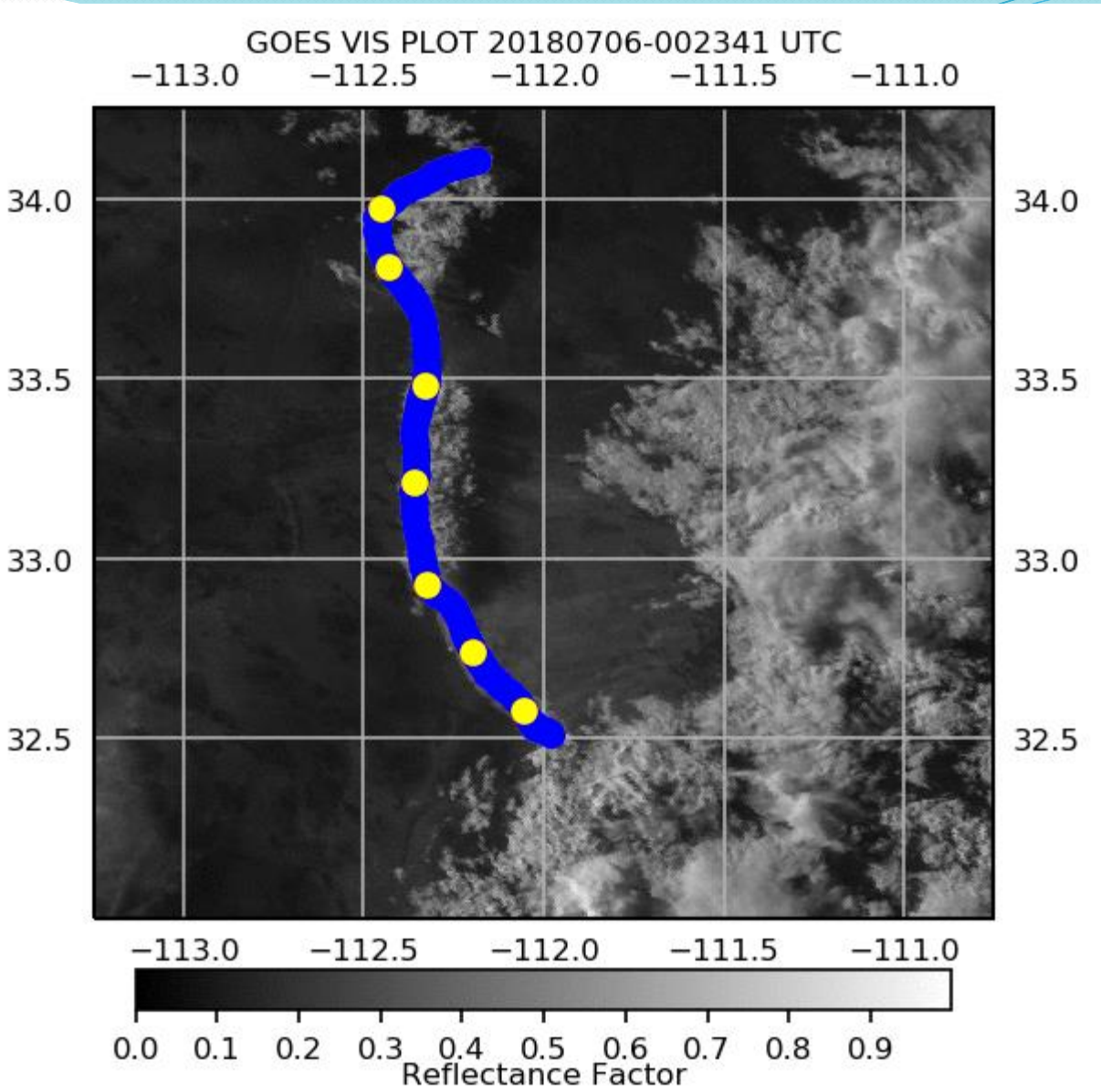

Figure 2. (Left) Example Brox et al. (2004) optical flow algorithm on 5-min GOES-16 visible imagery over central Arizona on 5 July 2018 (Right) Subjectively identified outflow boundary pixels tracked with old optical flow scheme (red/orange dots) compared to new scheme (blue/yellow dots). Note the scheme in blue and yellow preserves motion discontinuities.

Optical Flow at CIRA

- At CIRA we are testing 10 separate optical flow derivation techniques, and continue to develop new systems that leverage next-generation satellite fields
- Samples from two optical flow systems are shown here
  - Farnebäck (2001) from OpenCV (opencv.org)
    - Window: 5 x 5 pixels, local optimization window: 25x25 pixels
    - Pyramid Depth- 3 levels, Scaling- 0.5
    - Smoothing Std. Dev.- 1.0, Farnebäck Gaussian Smoothing Used
    - Sets $\boldsymbol{u} = [0,0]$ when no texture is available to find a solution!
  - A modified Sun et al. (2014) approach (more on the next slide)
- Applied to sequences and pairs of Geostationary and Low-Earth Orbiting Imagery
  - Typically track clouds/smoke/dust in Geostationary
  - Slower features in Low-Earth Orbiting Imagery (e.g. Sea Ice/Fire Lines)

Sun Et Al. (2014) Optical Flow

- New optical flow methods do handle Motion discontinuities, illumination changes, and texture-less regions, Brox et al. (2004) for example minimizes this with a coarse-to-fine strategy:

$$E(u(\boldsymbol{x}), v(\boldsymbol{x})) = \iint_{\Omega} \rho_d(BC + \gamma\, GC) + \alpha\, \rho_s(SC) d\boldsymbol{x}$$

BC = Brightness Constancy -> $|I(\boldsymbol{x} + \boldsymbol{U}, t + \Delta t) - I(\boldsymbol{x}, t)|^2$

GC = Gradient Constancy -> $|\nabla I(\boldsymbol{x} + \boldsymbol{U}, t + \Delta t) - \nabla I(\boldsymbol{x}, t)|^2$, γ = weight of GC → Mitigates motion caused by illumination changes

SC = Smoothness Constraint -> $|\nabla u|^2 + |\nabla v|^2$, α = weight of SC

The $\rho_d(x^2) = \rho_s(x^2) = \sqrt{x^2 + \varepsilon^2}$ are "Robust Functions" → Preserves motion discontinuities in image field

- We will use a method by Sun et al. (2014), minimizing:

$$E_{Sun}(u, v, \hat{u}, \hat{v}) = E(u, v) + \lambda_c(\|\boldsymbol{u} - \hat{\boldsymbol{u}}\|^2 + \|\boldsymbol{v} - \hat{\boldsymbol{v}}\|^2) + \lambda_n \sum_{i,j} \sum_{(i',j') \epsilon N_{i,j}} w_{i\,j}^{i'\,j'} \left(\left|\hat{u}_{i\,j} - \hat{u}_{i'\,j'}\right| + \left|\hat{v}_{i\,j} - \hat{v}_{i'\,j'}\right|\right)$$

Brox Equation

Coupling Term (penalizes deviations from auxiliary field $\hat{\boldsymbol{u}}$, $\hat{\boldsymbol{v}}$)

Weighted Median Smoothing Term (within a neighborhood of $N_{i,j}$)

- Resolves motion discontinuities
- Has aux. flow field which we can set to known values
- Weighted median can be based on GOES-R fields

$$w_{i\,j}^{i'\,j'} = e\text{^}\left\{-\frac{|i - i'|^2 + |j - j'|^2}{2\sigma_1^2} - \frac{\left|I_{i,j} - I_{i'\,j'}\right|^2}{2\sigma_2^2}\right\}$$

Sun Et Al. (2014) Optical Flow

- New optical flow methods do handle Motion discontinuities, illumination changes, and texture-less regions, Brox et al. (2004) for example minimizes this with a coarse-to-fine strategy:

$$E(u(\boldsymbol{x}), v(\boldsymbol{x})) = \iint_{\Omega} \rho_d(BC + \gamma\, GC) + \alpha\, \rho_s(SC)\, d\boldsymbol{x}$$

BC = Brightness Constancy -> $|I(\boldsymbol{x} + \boldsymbol{U}, t + \Delta t) - I(\boldsymbol{x}, t)|^2$
GC = Gradient Constancy -> $|\nabla I(\boldsymbol{x} + \boldsymbol{U}, t + \Delta t) - \nabla I(\boldsymbol{x}, t)|^2$, γ = weight of GC
SC = Smoothness Constraint -> $|\nabla u|^2 + |\nabla v|^2$, α = weight of SC
The $\rho_d(x^2) = \rho_s(x^2) = \sqrt{x^2 + \varepsilon^2}$ are "Robust Functions"

Params. that can be tuned

- We will use a method by Sun et al. (2014), minimizing:

$$E_{Sun}(u, v, \hat{u}, \hat{v}) = E(u, v) + \lambda_c(\|\boldsymbol{u} - \hat{\boldsymbol{u}}\|^2 + \|\boldsymbol{v} - \hat{\boldsymbol{v}}\|^2) + \lambda_n \sum_{i,j} \sum_{(i',j') \epsilon N_{i,j}} w_{i\,j}^{i'\,j'} \left(\left|\hat{u}_{i\,j} - \hat{u}_{i'\,j'}\right| + \left|\hat{v}_{i\,j} - \hat{v}_{i'\,j'}\right|\right)$$

Brox Equation

Coupling Term (penalizes deviations from auxiliary field $\hat{\boldsymbol{u}}$, $\hat{\boldsymbol{v}}$)

Weighted Median Smoothing Term (within a neighborhood of $N_{i,j}$)

- Resolves motion discontinuities
- Has aux. flow field which we can set to known values
- Weighted median can be based on GOES-R fields

$$w_{i\,j}^{i'\,j'} = e\text{^}\left\{-\frac{|i - i'|^2 + |j - j'|^2}{2\sigma_1^2} - \frac{\left|I_{i,j} - I_{i'\,j'}\right|^2}{2\sigma_2^2}\right\}$$

Little to no texture in the ocean at 0.64-µm channel

Approaches that fail here:

- Farnebäck
- Patch Matching & Cross Correlation (DMWs/AMVs)
- Lucas and Kanade

Approaches that would over-smooth:

- Farnebäck
- Brox et al. (2004)
- Horn and Schunck
- Bruhn et al. (2005)
- Black and Anandan (1994)

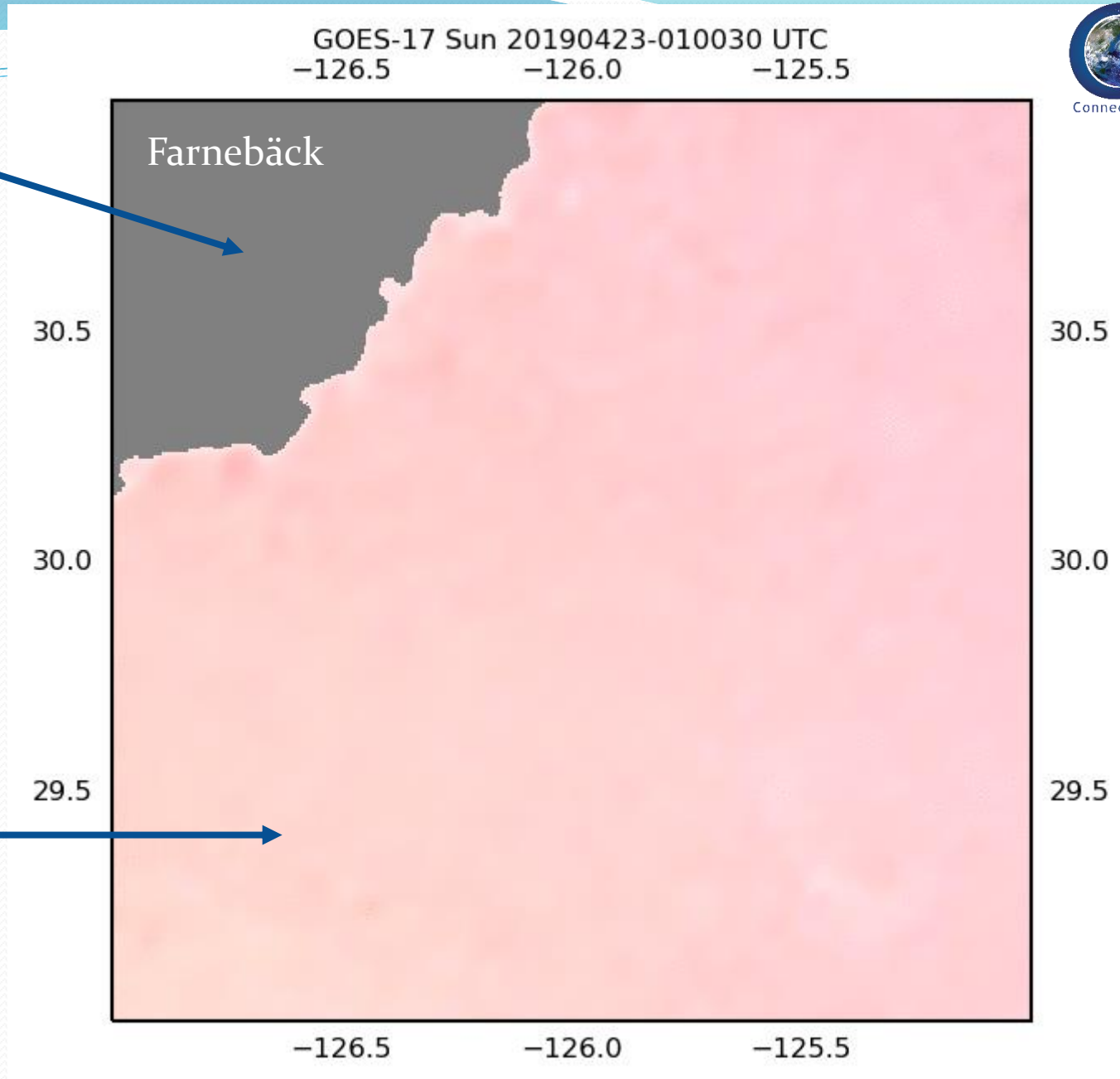

Auxiliary field was used where "ocean" pixels were detected, set to stationary, yields unmatched texture in passive geostationary satellite motion fields

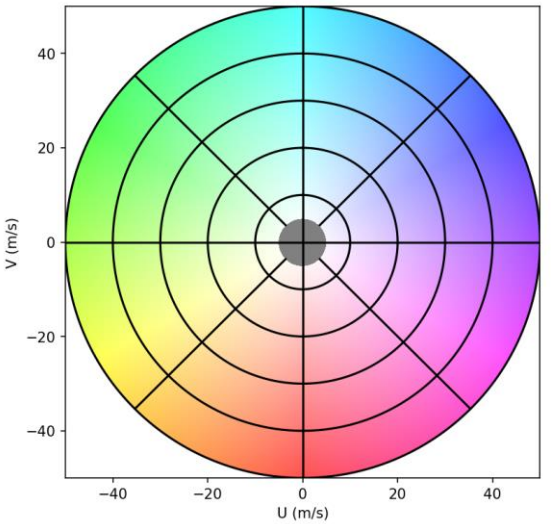

Figure 3. Cumulus optical flow example over the Pacific Ocean of GOES-17 0.64-µm 1-min imagery.

Applications

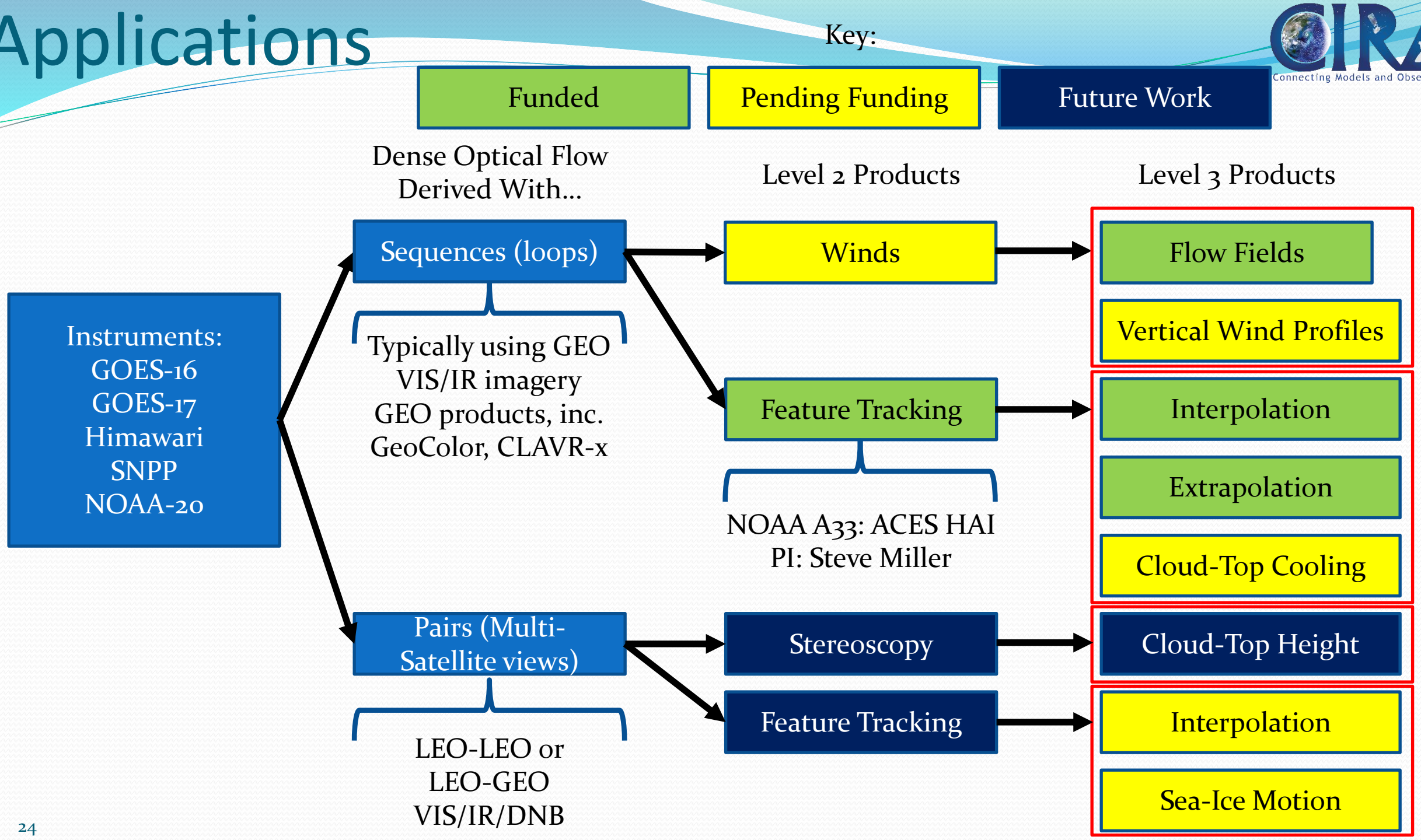

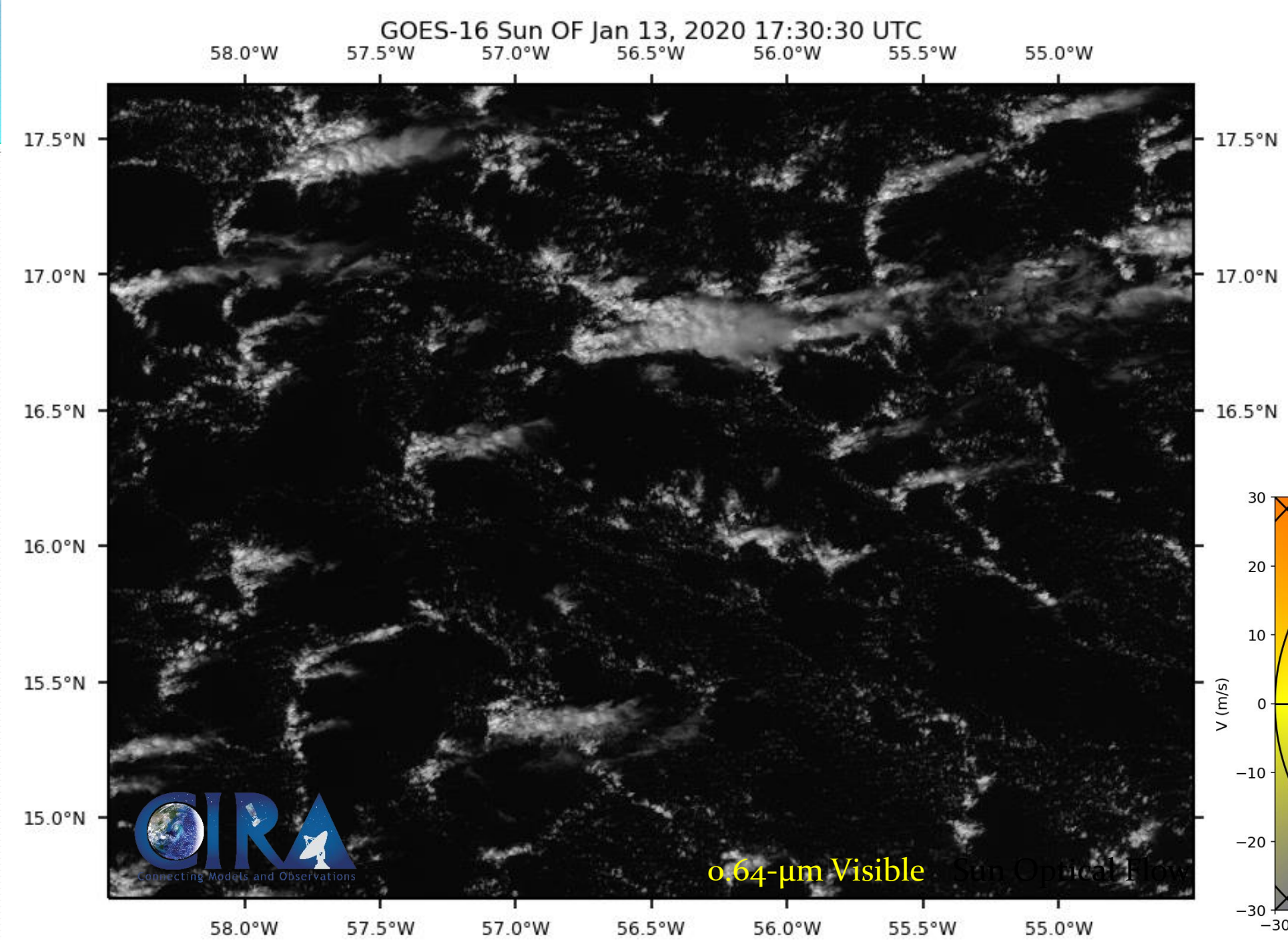

- Dense optical flow meso-winds products see vertical growth in clouds as acceleration in cloud-top horizontal motion, see color scale below (where grey=stationary)
- Hodograph (below) indicates GFS analysis wind speed and direction as a function of height for this scene

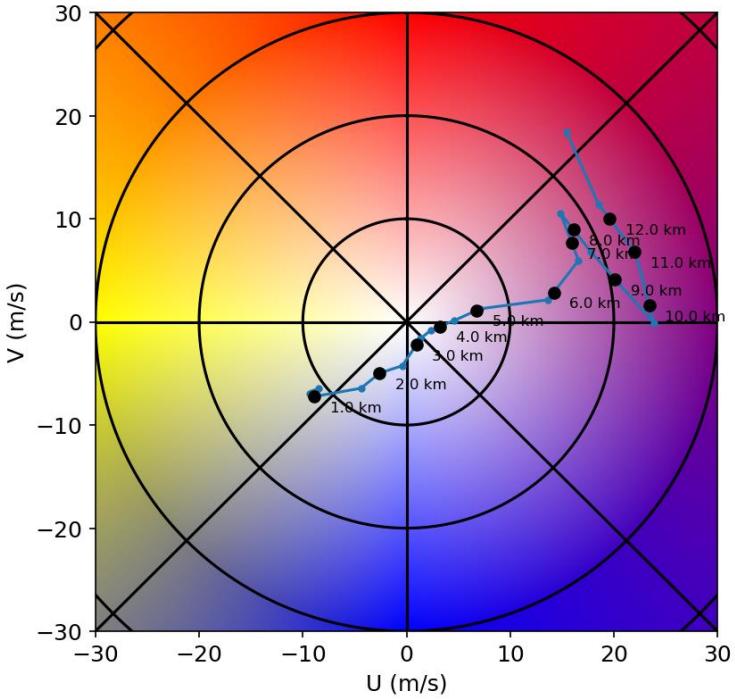


Dense optical flow enables temporal interpolation of satellite imagery (e.g. 1-min GeoColor updates from GOES 5-min CONUS data)

DNB Imagery

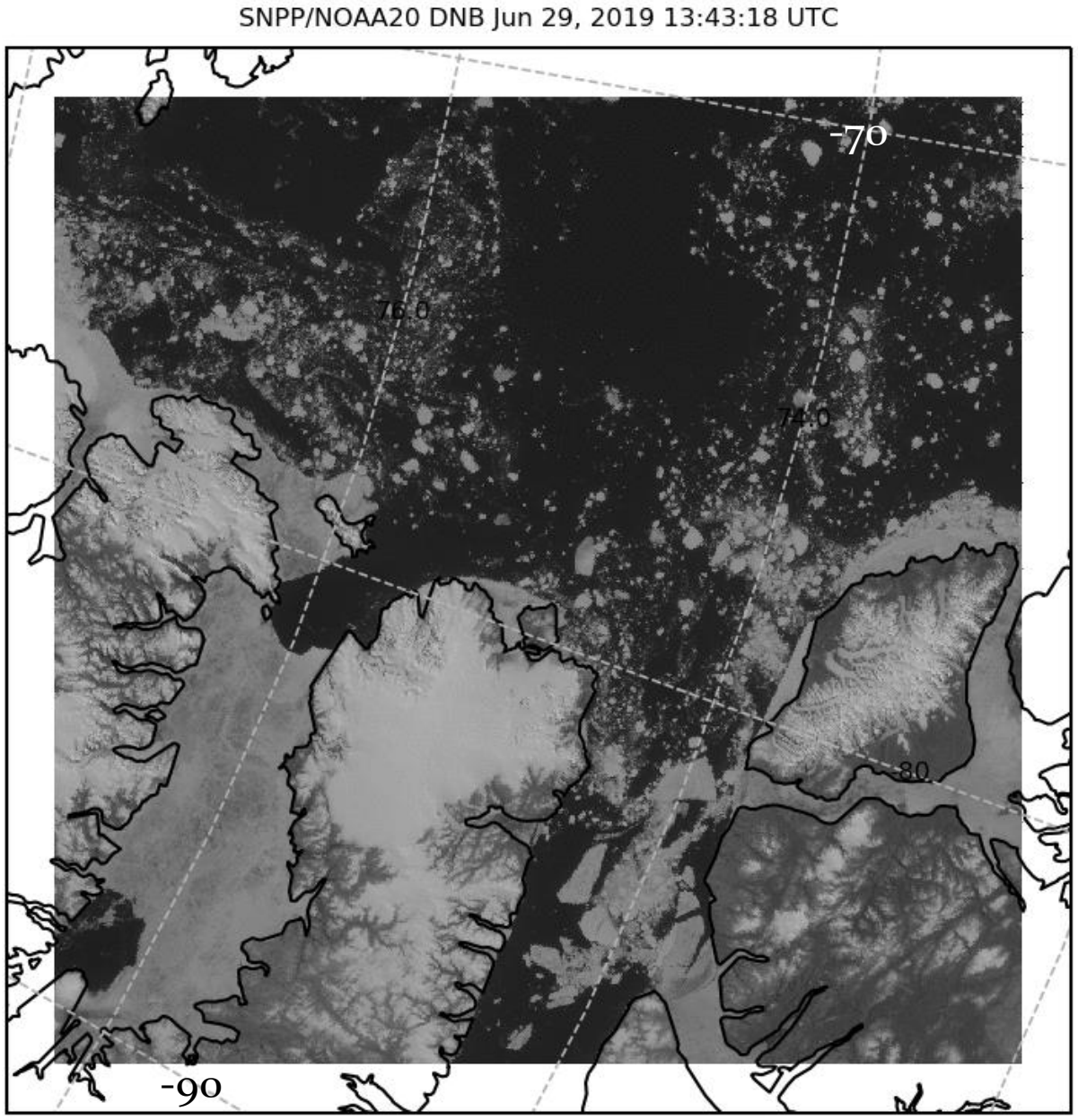

Color-Shaded Optical Flow Comparison

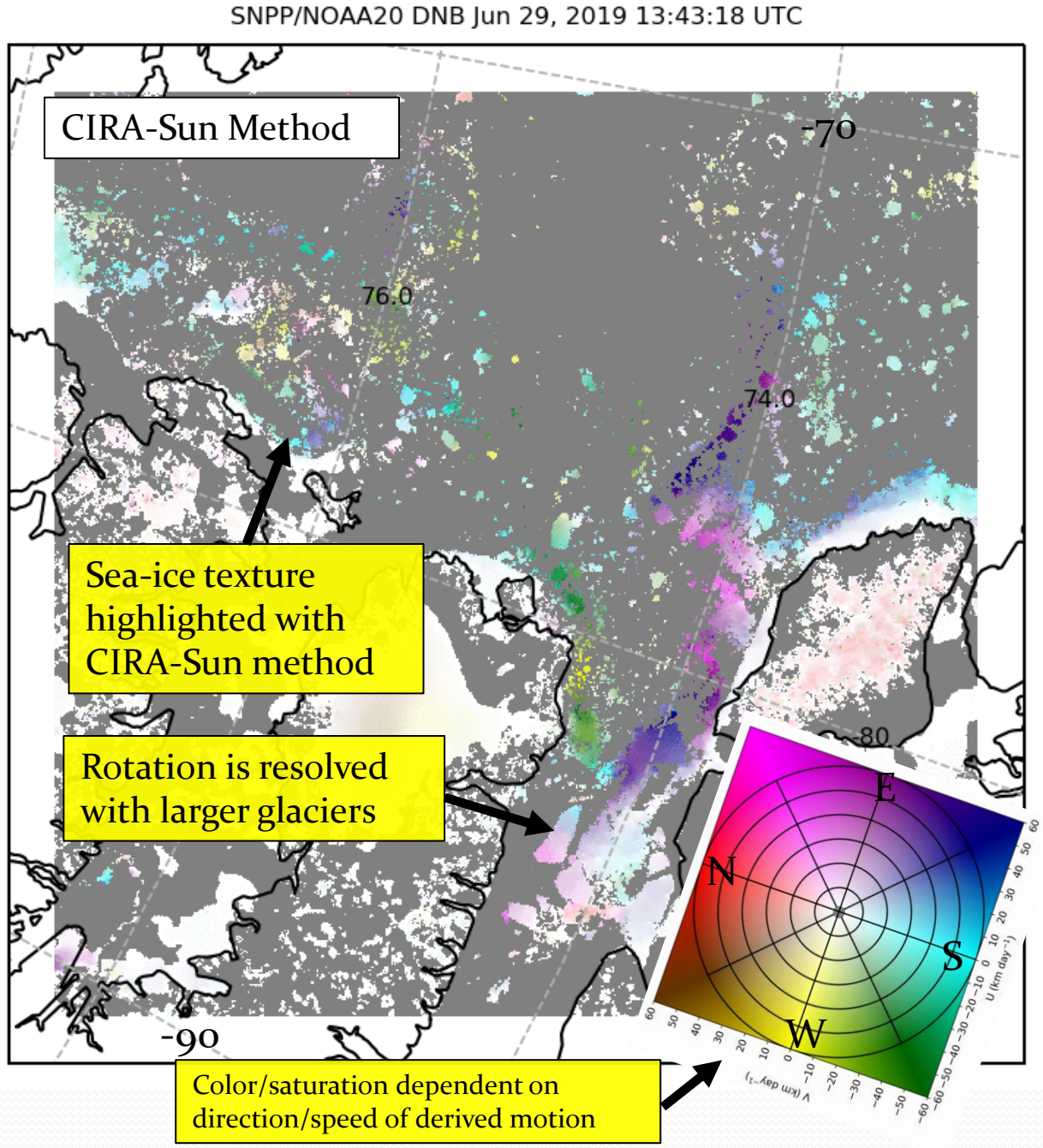

Cloud-Top Cooling

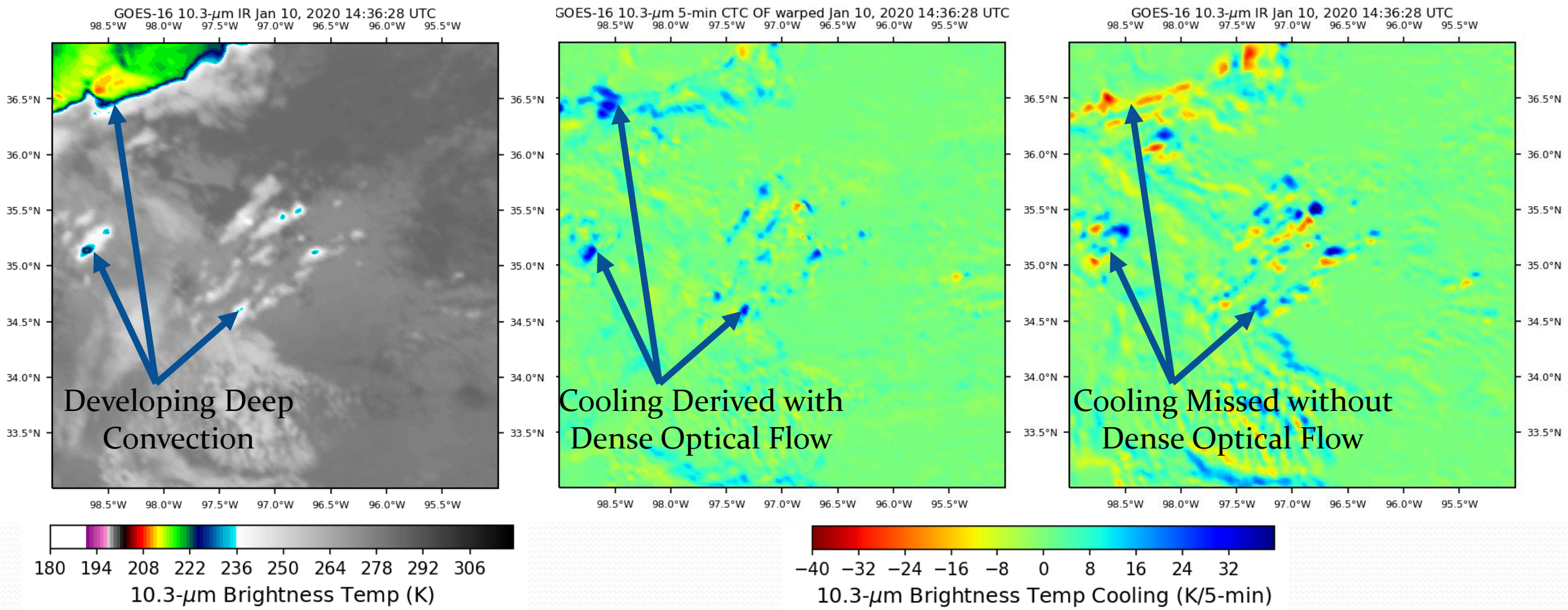

*Time-rates of change can *dramatically* complement the native 16-channels on GOES-R ABIs for AI/Machine Learning

Optical Flow Validation

- Application development is closely tied to optical flow validation
- There are two key methods to validate optical flow (e.g. Baker et al. 2011):

1) Validation with Wind Measurements
   - In many applications, it is assumed that optical flow = winds
   - Winds can be validated with in situ measurements (rawinsondes) or remote sensing tools (e.g. Doppler Radar/Lidar) wind profilers nearby in space/time
   - Key disadvantage: Not all brightness features move w/ the wind motion
     - E.G. gravity waves, surface features, outflow boundaries

2) Validation with Image Interpolation
   - In many other applications, it may be beneficial to better track features
   - Optical Flow estimates can be combined with a simple interpolation algorithm to estimate intermediate frames and evaluate feature tracking performance
     - Performance is determined by comparing estimated image to a known image typically with a gradient normalized sum-of-square error
     - In most cases, this can be done w/ 1-min and 30-sec mesoscale sectors

Citation: Baker, S., D. Scharstein, J. P. Lewis, S. Roth, M. J. Black, and R. Szeliski, 2011: A database and evaluation methodology for optical flow. *Int. J. Comput. Vis.*, **92**, 1–31, doi:10.1007/s11263-010-0390-2.

Initial Validation Results

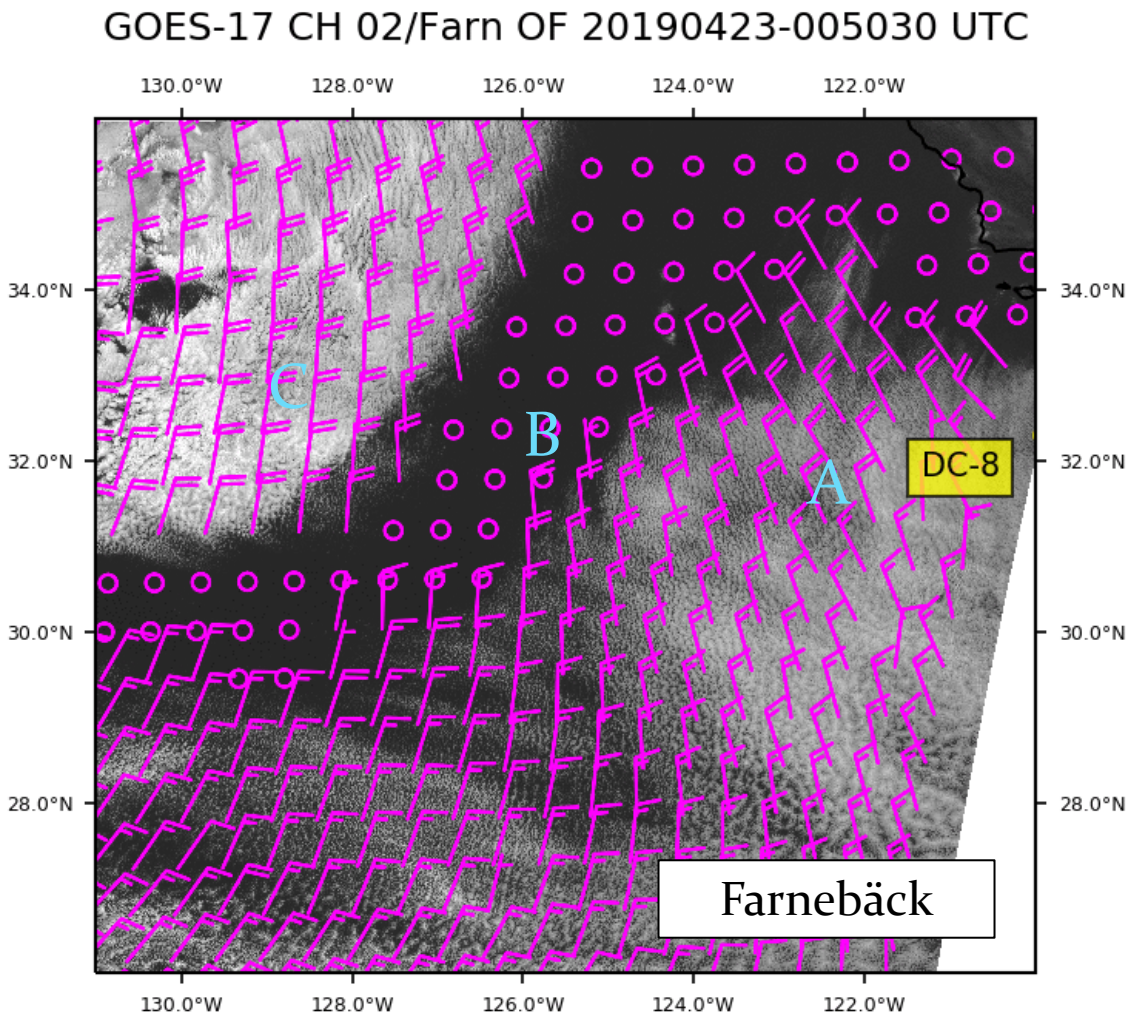

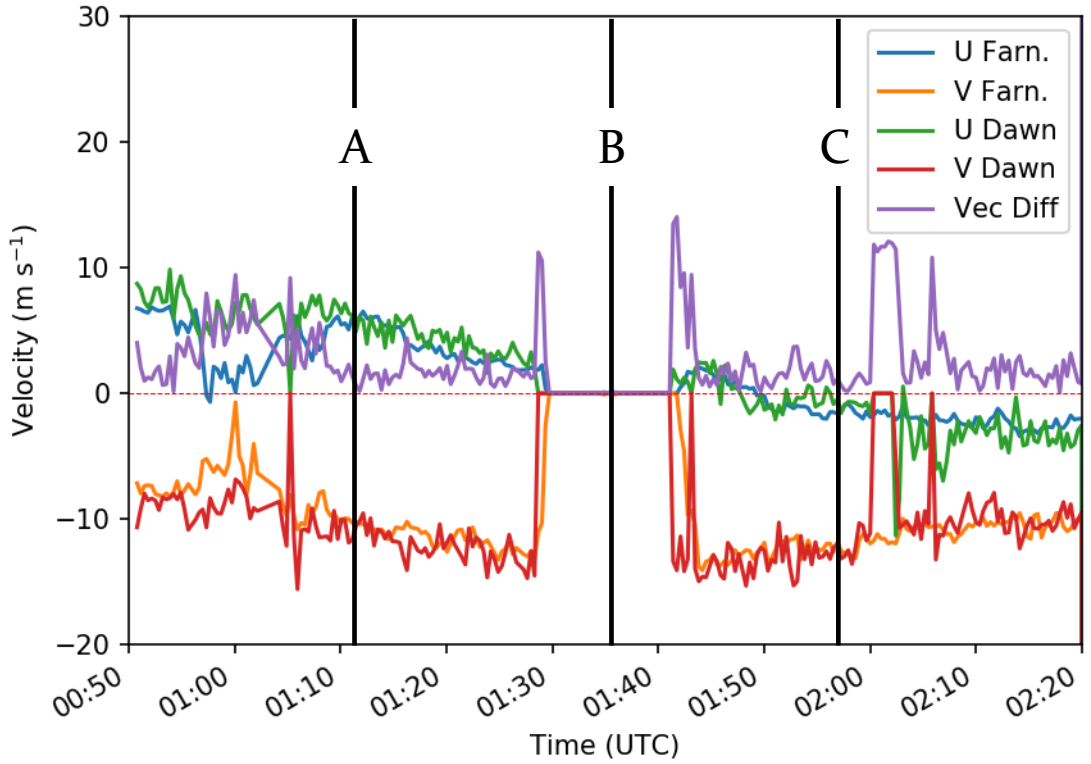

Figure 3. GOES-17 Ch-02 0.64 μm imagery plotted with Farnebäck optical flow. Below is a time series comparison of the Farnebäck optical flow approach validation when compared with the DAWN wind profiler on board the DC-8, whose path is traced on the satellite image.

- With visible information, dense flow field is VERY close to Doppler wind-profiling Lidar data (DAWN) w/ cloud-top assumed at SNR > 10 (errors ~< 5 m/s)
- Spikes in vector differences occur when lidar/optical flow disagree on discontinuity locations

Validation

Table 1. Initial dense optical flow validation statistics when compared to NASA DAWN Wind Profiling Lidar

Algorithm	Bias (m s^{-1})*	Mean Vector Difference (m s^{-1})*
Sun et al. (2013) (IR Ch-7)	1.623	4.04
Modified-Sun et al. (2013) (IR Ch-7)	-0.798	3.101
Farnebäck (2001) (visible imagery)	-0.597	2.447
-> Modified 1-min (2 Pyr. levels)	-0.114	2.272
-> 3 min | 5 min | 10 min	-0.15| 0.15 | -1.91	2.327|2.068|4.38
DMW's (IR Ch-7) from Daniels et al. (2018)**	< |-0.5|	~2.9-4.5
DMW's (visible Ch-2) from Daniels et al. (2018)**	< |0.5|	~2.8-3.7

- 1-min MVD can be lower w/ INR correction
- 10-min requires additional modification, doesn't perform as well as finer temporal resolutions

* Values for Sun et al., modified Sun et al. and Farneback assume winds were derived at Lidar derived cloud-top height and should be considered preliminary, no height assignment was performed yet

** Values for DMWs were height assigned and compared to rawinsondes, not DAWN

Daniels, J., W. Bresky, A. Bailey, A. Allegrino, S. Wanzong and C. Velden, 2018: Introducing Atmospheric Motion Vectors Derived from the GOES-16 Advanced-Baseline Imager. *14th Annual Symposium on New Generation Operational Environmental Satellites,* Austin, TX, Amer. Meteor. Soc.

Meso-Winds Working Group

Slide Courtesy of
Jaime Daniels (NOAA/NESDIS/STAR)

Member	Affiliation
Jaime Daniels (Chair)	NESDIS/STAR, College Park, MD
Chris Velden (Chair)	Univ. of Wisconsin/CIMSS
Wayne Bresky	IMSG, Inc.
Andrew Bailey	IMSG, Inc.
Steve Wanzong	Univ. of Wisconsin/CIMSS
Dave Stettner	Univ. of Wisconsin/CIMSS
Dave Santek	Univ. of Wisconsin/CIMSS
Jason Apke	CIRA
Thomas Vandal	NASA-Ames
Kris Bedka	NASA Langley
Bob Rabin	NOAA/NSSL

Goals of this working group:

- Increase collaborations between those doing work on meso-AMVs
- Leverage collaborations to share and test new approaches, algorithms, and applications on common datasets
- Identify maturing approaches and applications that may be suited for operationalization
- Actively engage and collaborate with potential users of mesoscale AMVs

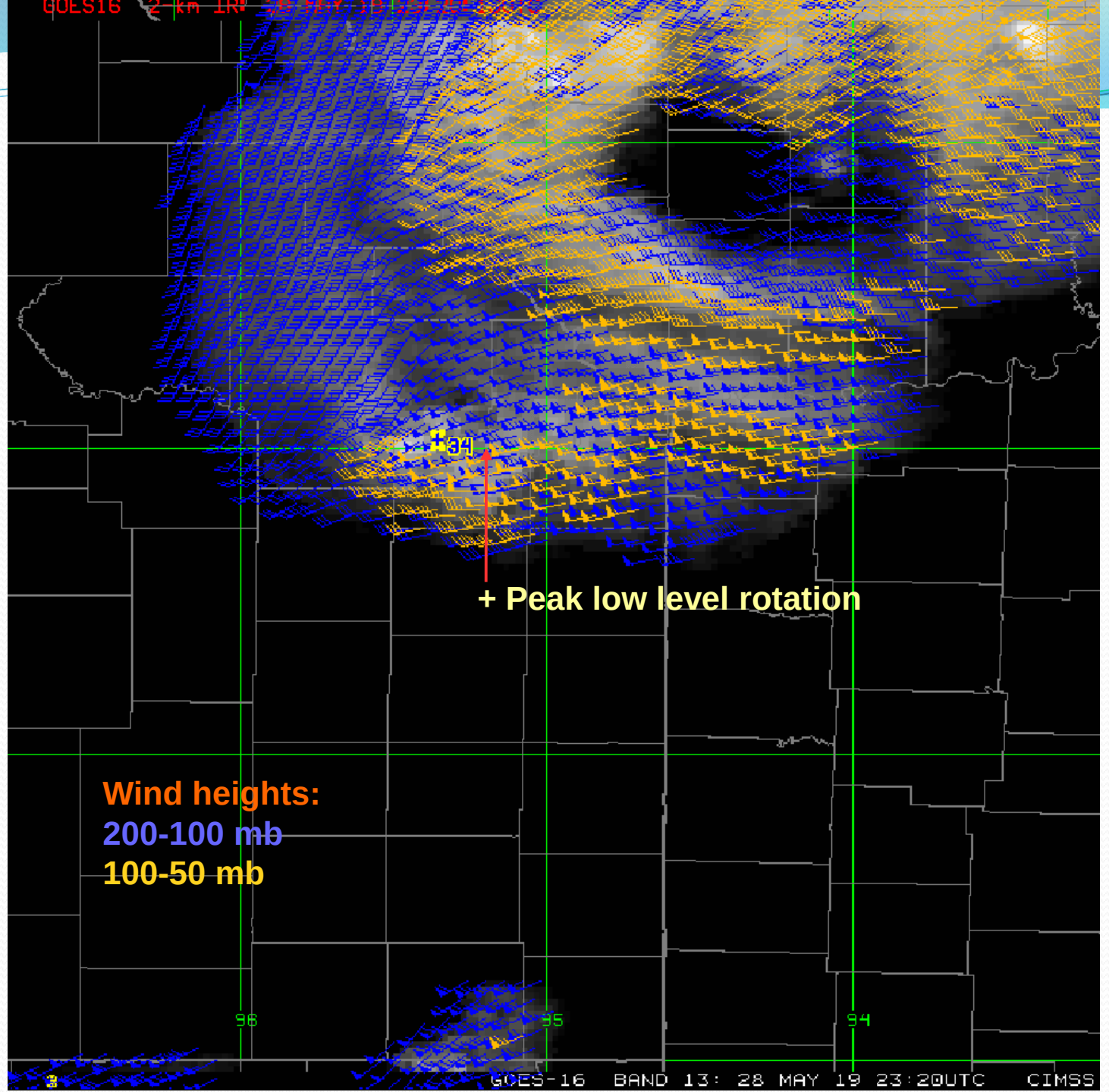

Courtesy:
Bob Rabin (NOAA/NSSL)

OF Applications to Tropical Cyclones

Project Goals: Develop ultrahigh spatiotemporal atmospheric motion vector (AMV) datasets derived from the new-generation GOES-R series ABI meso scans targeting tropical cyclones (TCs), and optimize their assimilation into TC forecast models.

UWisc.-CIMSS Contributors:

Christopher Velden, David Stettner, Steven Wanzong, Will Lewis

NOAA/University Collaboration Partners:

AMV Development - Robert Rabin, NSSL; Jaime Daniels, NESDIS/STAR
Hurricane DA - Jason Sippel, NOAA/HRD; Xuguang Wang, OU

Stakeholders and End Users: NHC, CPHC, JTWC TCFOs; NCEP/EMC TC models

One Project Objective:

- Demonstrate new OF methodology for producing AMVs in hurricane environments to augment and enhance existing techniques; Focus on the very cold and relatively coherent clouds in the Central Dense Overcast (CDO) region of TCs where conventional AMV techniques can struggle.

Nearing end of methodology/product development stage

- Proof of concept completed through case studies and publications
- Successful completion of real-time demo with GOES-16 during 2020 TC season
- Data quality/validation studies ongoing
- Data assimilation activities underway with modeling partners (i.e. HWRF model)

Readying product for transition to Enterprise system implementation and testing with STAR partners

Product Example: Hurricane Delta

(OF vectors in magenta)

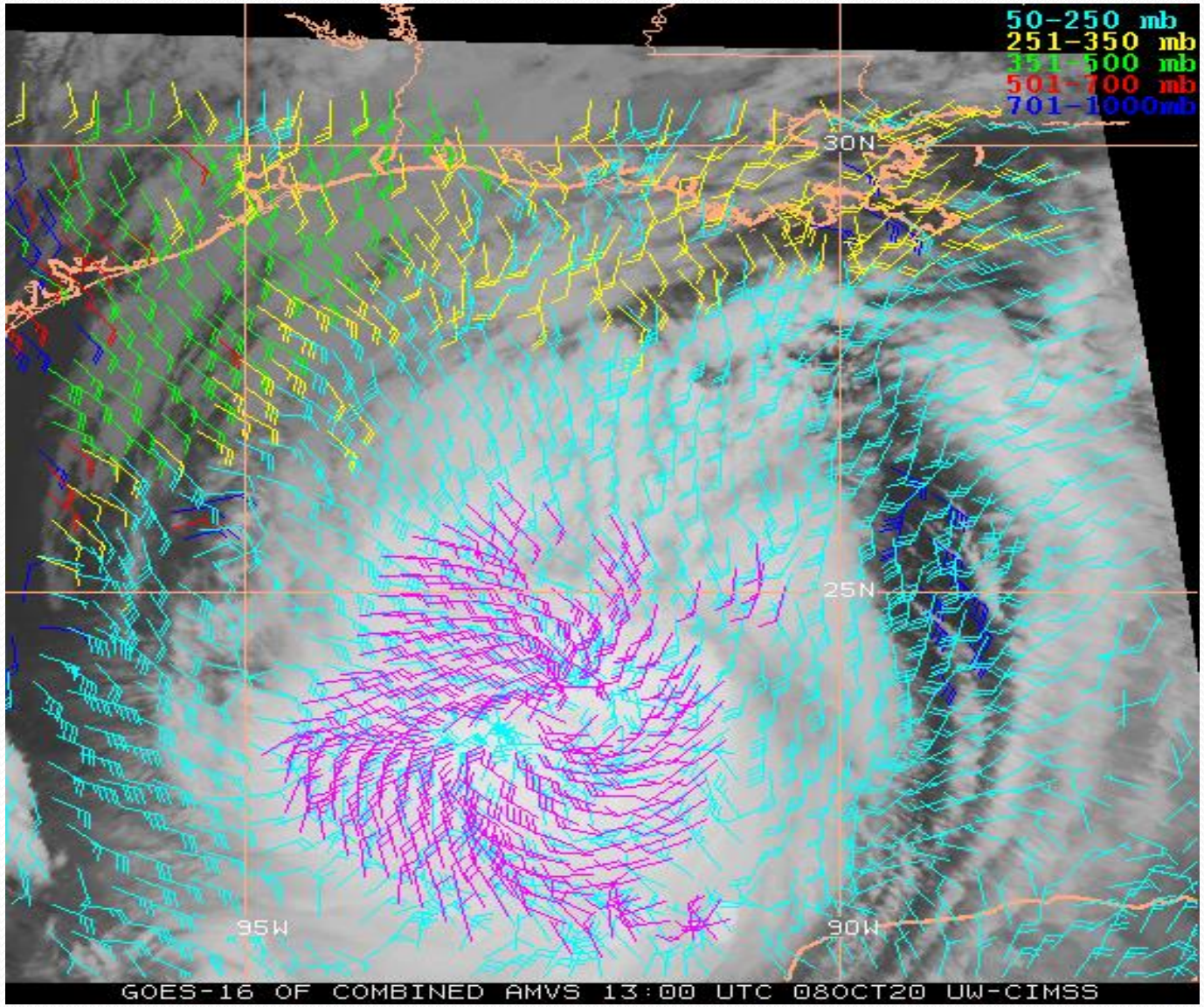

Courtesy:
Chris Velden (UW-CIMSS)

Machine Learning based Optical Flow for Quantifying Motion

- Deep learning methods are widely accepted for optical flow in the computer vision community
- Research is underway to test neural networks with false color imagery to retrieve optical flow within clouds
- Applied to temporal interpolation of geostationary imagery to generate 1-minute full-disk data
- Proposal selected by NASA ROSES Earth Science Research from Operational Geostationary Satellite Systems Program (Thomas Vandal, Will McCarty)

False Color Image

Wind Speed

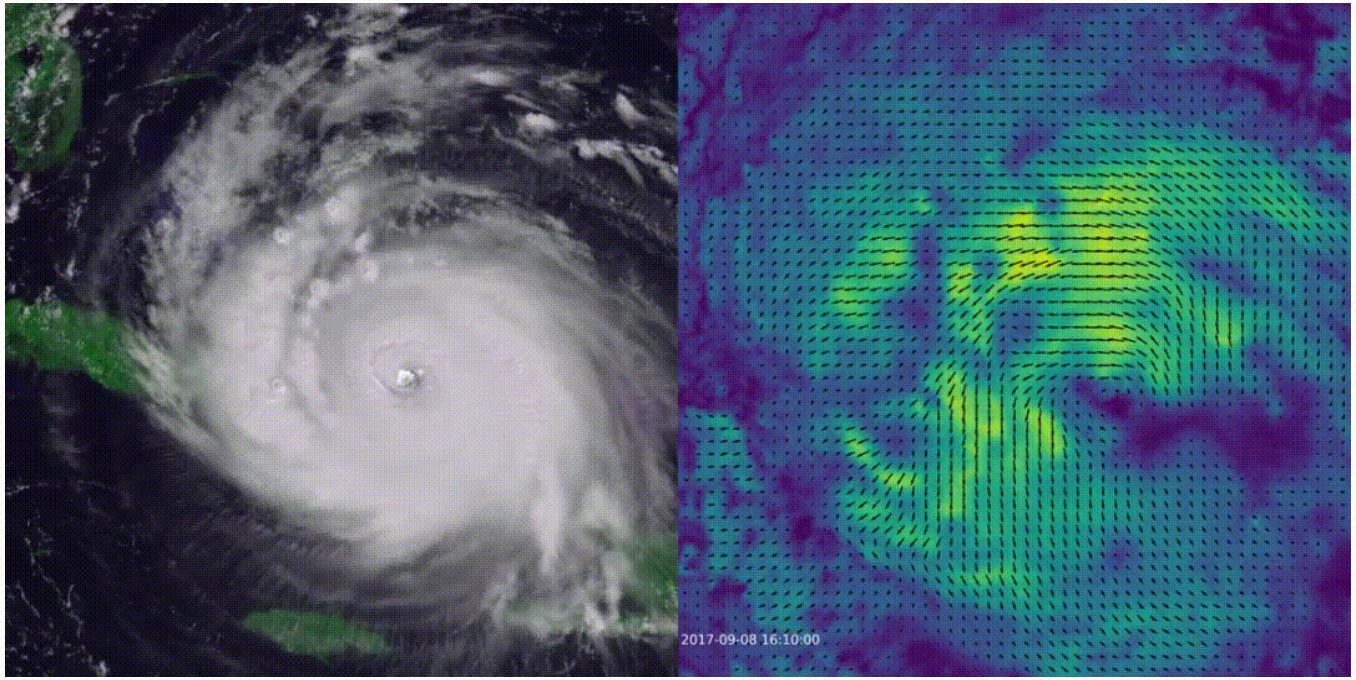

Vandal, T. & Nemani, R. (2020). “Optical Flow for Intermediate Frame Interpolation of Multispectral Geostationary Satellite Data”. 1st ACM SIGKDD Workshop on Deep Learning for Spatiotemporal Data, Applications, and Systems.

Courtesy: Thomas Vandal (NASA Ames)

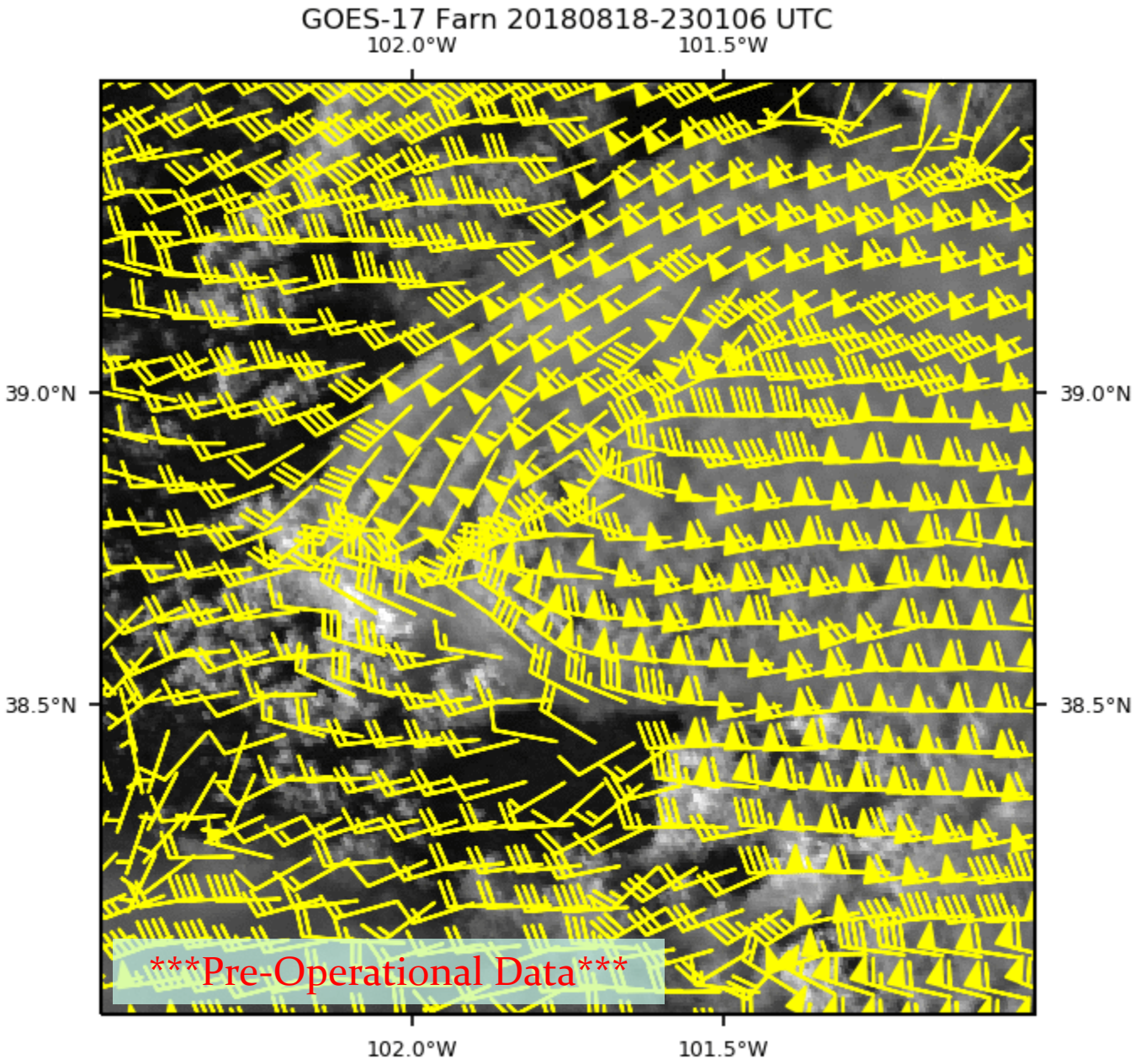

Courtesy: Dan Lindsey (NOAA)

A look into the future

- While GOES-17 was in the checkout phase, a ~6 s rapid scan test was performed over hail-producing t-storms
- MYTH: Motions can only be derived from satellite data if they exceed 1-pixel
- FACT: Optical flow algorithms, including sparse cross-correlation based AMVs/DMWs can derive sub-pixel motions. The actual "speed limit" is determined by the horizontal gradient in image brightness and the radiometric resolution of the image***
- Farnebäck (2001), for example, produces realistic motions when two frames only ~6 seconds apart are used!
- FACT: Optical flow algorithms perform poorly when image changes occur that are NOT related to movement (clouds change more between images with lower scan rates!)

To Summarize…

- We reviewed methods for sparse and dense optical flow computation
  - GOES-R enables assumptions within dense optical flow retrieval algorithms!
- Introduced a dense optical flow method which leverages GOES-R fields for better flow solutions
- Demonstrated several applications of dense optical flow fields
  - Winds/Feature Tracking/Interpolation
- Showed early validation results in comparison to Doppler Wind Lidar data
  - Winds products have comparable accuracy to state-of-the-art algorithms
  - Accuracy degrades as temporal resolution is coarsened (≥ 10 min)
- Future plans include
  - More validation and testing in a variety of meteorological phenomena
  - Continue development on current algorithms and image interpolation schemes (NOAA ROSES A33- ACES-HAI; PI- Steve Miller)

Acknowledgements

- Work was funded under NESDIS GOES-R Program Office award number: NA14OAR4320125, and by the Multidisciplinary University Research Initiative (MURI) grant N00014-16-1-2040.

Citations

Apke, J. M., J. R. Mecikalski, and C. P. Jewett, 2016: Analysis of Mesoscale Atmospheric Flows above Mature Deep Convection Using Super Rapid Scan Geostationary Satellite Data. *J. Appl. Meteorol. Climatol.*, **55**, 1859–1887, doi:10.1175/JAMC-D-15-0253.1. http://journals.ametsoc.org/doi/10.1175/JAMC-D-15-0253.1.

——, ——, K. M. Bedka, E. W. McCaul Jr., C. R. Homeyer, and C. P. Jewett, 2018: Relationships Between Deep Convection Updraft Characteristics and Satellite Based Super Rapid Scan Mesoscale Atmospheric Motion Vector Derived Flow. *Mon. Wea. Rev.*, **146**, 3461–3480. https://doi.org/10.1175/MWR-D-18-0119.1.

Brox, T., A. Bruhn, N. Papenberg, and J. Weickert, 2004: High accuracy optical flow estimation based on a theory for warping. *2004 Eur. Conf. Comput. Vis.*, **4**, 25–36.

Farnebäck, G., 2001: Two-Frame Motion Estimation Based on Polynomial Expansion. *Proceedings: Eighth IEEE International Conference on Computer Vision*, Vol. 1 of, 171–177.

Fortun, D., P. Bouthemy, C. Kervrann, D. Fortun, P. Bouthemy, and C. Kervrann, 2015: Optical flow modeling and computation : a survey To cite this version : Optical flow modeling and computation : a survey. *Comput. Vis. Image Underst.*, **134**, 1–21. https://hal.inria.fr/hal-01104081/file/CVIU_survey.pdf.

Horn, B. K. P., and B. G. Schunck, 1981: Determining optical flow. *Artif. Intell.*, **17**, 185–203, doi:10.1016/0004-3702(81)90024-2.

Sun, D., S. Roth, and M. J. Black, 2014: A quantitative analysis of current practices in optical flow estimation and the principles behind them. *Int. J. Comput. Vis.*, **106**, 115–137, doi:10.1007/s11263-013-0644-x.

Wu, Q., H.-Q. Wang, Y.-J. Lin, Y.-Z. Zhuang, and Y. Zhang, 2016: Deriving AMVs from Geostationary Satellite Images Using Optical Flow Algorithm Based on Polynomial Expansion. *J. Atmos. Ocean. Technol.*, **33**, 1727–1747, doi:10.1175/JTECH-D-16-0013.1. http://journals.ametsoc.org/doi/10.1175/JTECH-D-16-0013.1.

Thank You For Listening!

For additional questions, contact:

Jason Apke

jason.apke@colostate.edu

3925A West Laporte Ave. Fort Collins, CO 80523-1375

EXTRA SLIDES

For additional questions, contact:

Jason Apke

jason.apke@colostate.edu

3925A West Laporte Ave. Fort Collins, CO 80523-1375

Doppler Aerosol Wind (DAWN) Lidar System

PI: Michael J. Kavaya, NASA LaRC

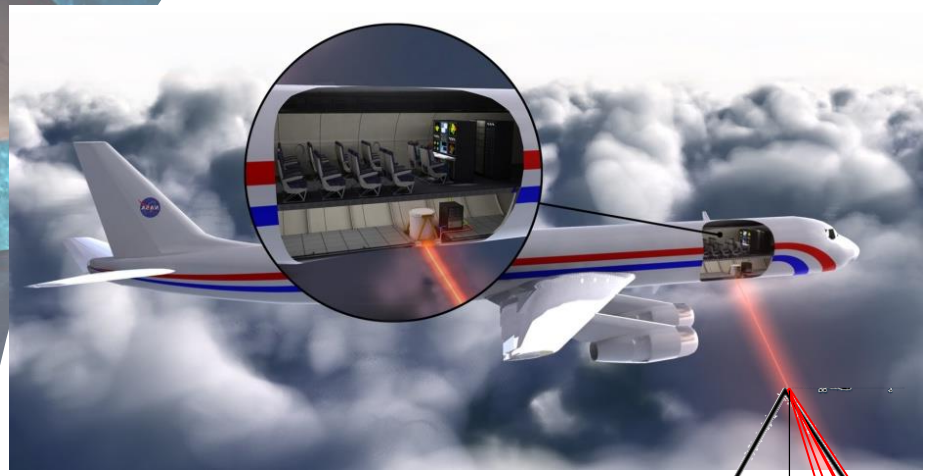

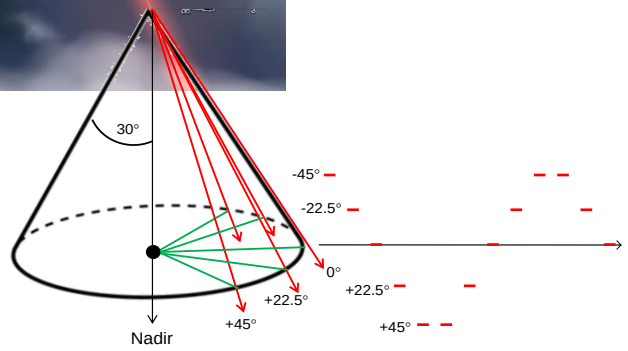

Attribute	Value
Airplanes Flown	DC-8 and UC-12B
Solid-State Laser Crystal and Wavelength	Ho:Tm:LuLiF, 2.053 Microns
Laser Architecture	Master Oscillator Power Amplifier (MOPA)
Pumping Source, Wavelength, Duration	Laser Diode Arrays (LDA), 792 nm, 1 ms
Laser Pulse Energy E, Rate f, FWHM Duration t	80-100 mJ, 10 Hz, 180 ns
Telescope Diameter D	15 cm
Light Detection Material, Technique	InGaAs, Coherent, Dual-Balanced
Scanner Diameter, Type, Deflection	15 cm, Step-Stare Rotating Wedge, 30° About Nadir
Eye Safety	Safe at any Range When DAWN Closed Up for Flight
Pointing Knowledge Technique	Dedicated INS/GPS on Lidar; dry land returns
LOS Wind Measurement Precision	< 1 m/s
Vertical Resolution	60 m

Precision = < 1 m/s

DAWN Capabilities

- 2.053 micron wavelength, 80-100 mJ/pulse. High sensitivity to aerosol backscatter, enables excellent vertical resolution, accuracy, and atmospheric coverage
- Provides vertical profiles of LOS wind, horizontal wind vectors, and aerosol backscatter
- Optional number of azimuth angles (up to 12) permits trade of wind variability determination vs. horizontal resolution
- Optional number of laser shots averaged for each LOS wind profile permits trade of atmospheric coverage vs. horizontal resolution
- Data may be processed multiple ways to provide various combinations of vertical and horizontal resolution, atmospheric coverage, and accuracy
- Successful field campaigns: Polar Winds I and II, Convective Processes Experiment (CPEX), ADM Aeolus Cal/Val Test Flight Campaign

Initial Validation Results- Sun

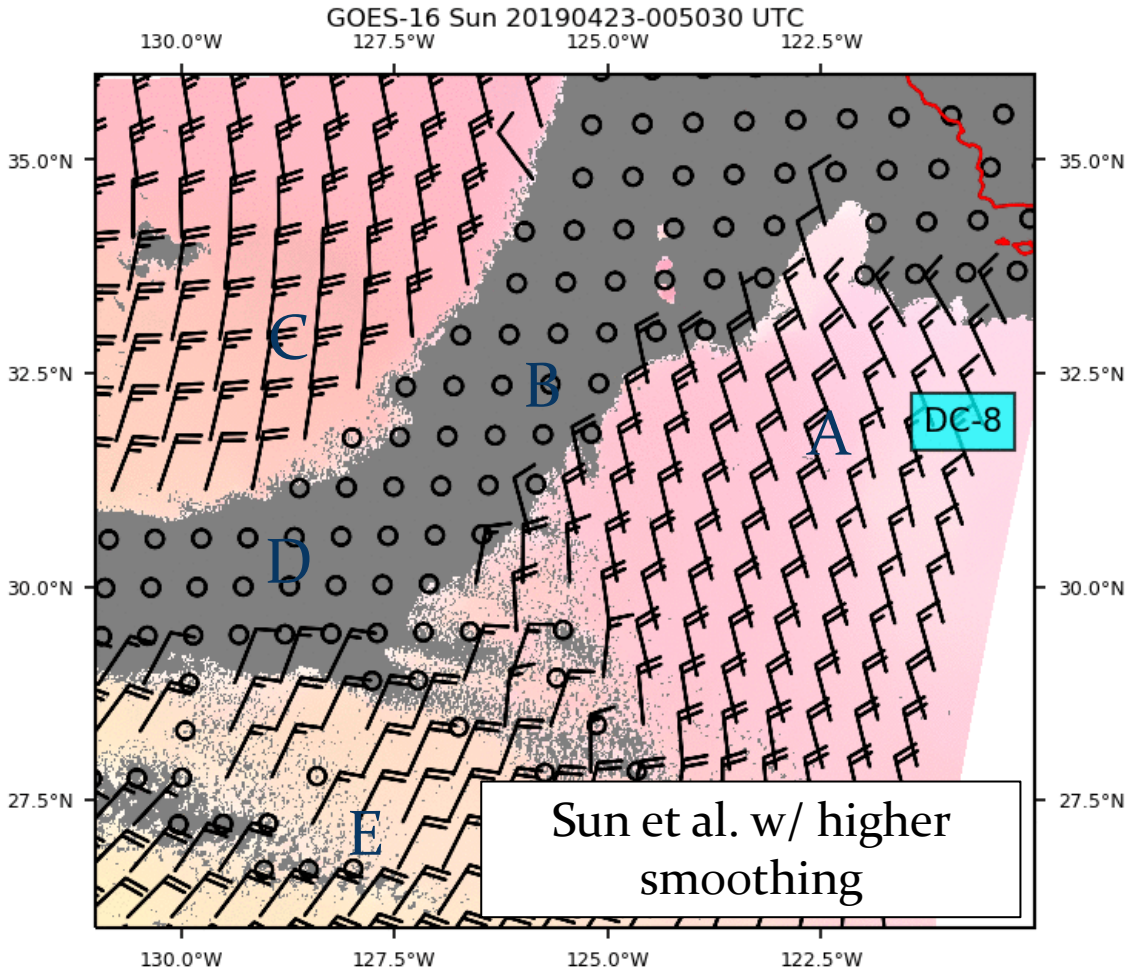

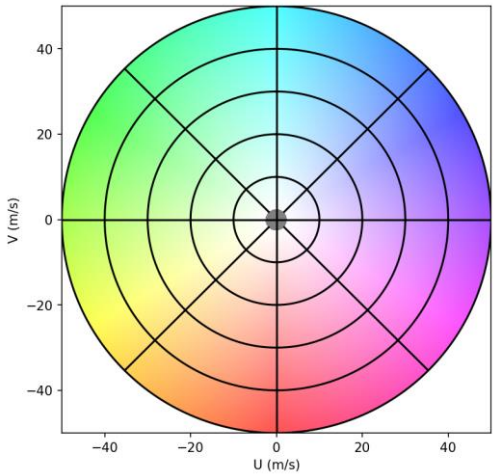

Figure 3. GOES-17 Ch-07 3.9 µm imagery plotted with Sun optical flow vectors tuned without and with an auxiliary stationary flow field for clear/ground/ocean pixels. Also shown is a color shaded optical flow plot, where hue is determined by direction, and saturation by the speed of the flow. Below is a time series comparison of the Sun optical flow approach validation when compared with the DAWN wind profiler on board the DC-8, whose path is traced on the satellite image.

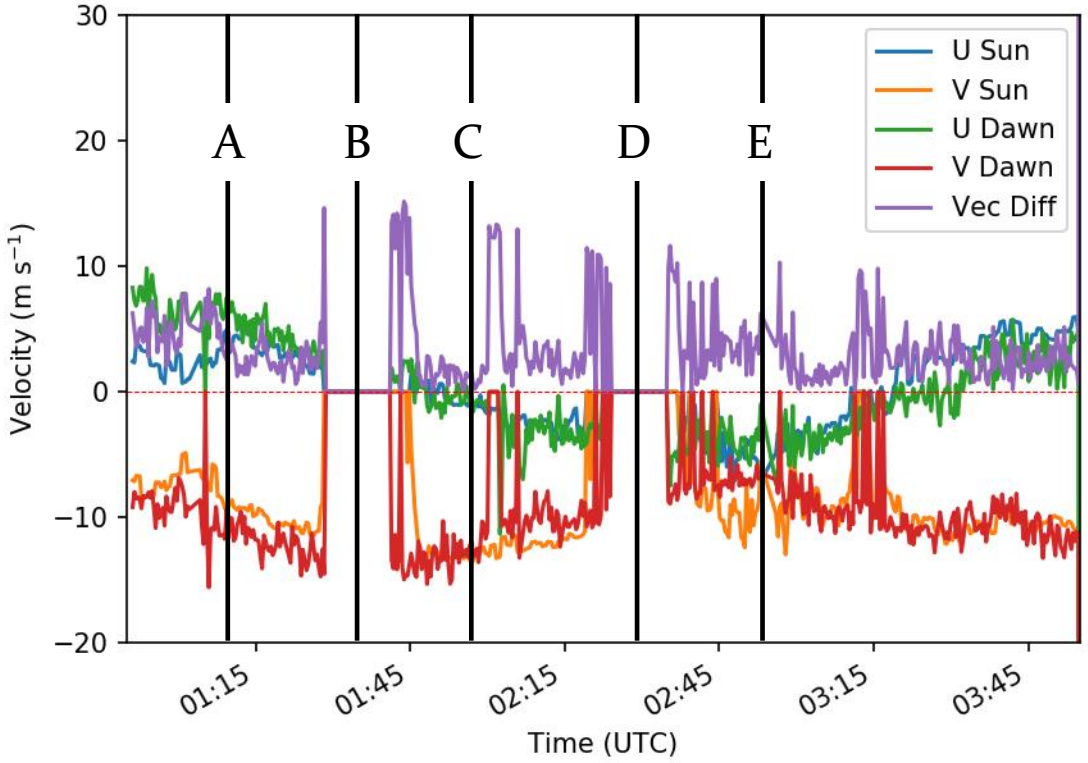

- Points B and D are over the ocean, which requires auxiliary tuning to get stationary motion
- Tuning yields correct stationary motion at B and D
- Noise before A and during E still needs tuning
- Field behaves well around point C, errors < 3 m/s

Validation: 4/25/2019 Part I

- Dense Optical Flow approaches handle motion of closed-cell convection very well, w/ vector differences around ~1.5 m s^{-1} , Bias < 0.1 m s^{-1}
- Approaches struggle to match DAWN wind speeds in multi-motion cirrus (after 22:40 UTC)
  - Cirrus is at DAWNs highest range gate, so it is possible actual motion was higher in altitude than what was measured
  - Sun/Apke Optical Flow Algorithm shows signs of mixing multiple motions, which could be a side effect of computational efficiency steps
- Improvements will be made by leveraging multi-channel approaches and CLAVR-x cloud-top heights

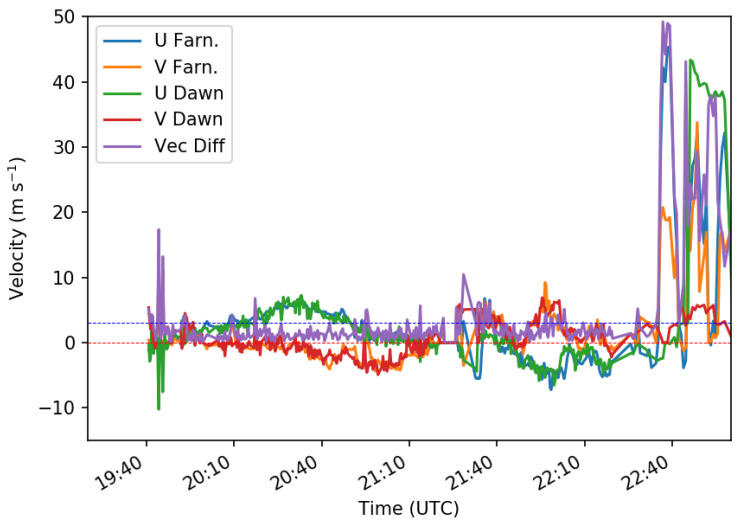

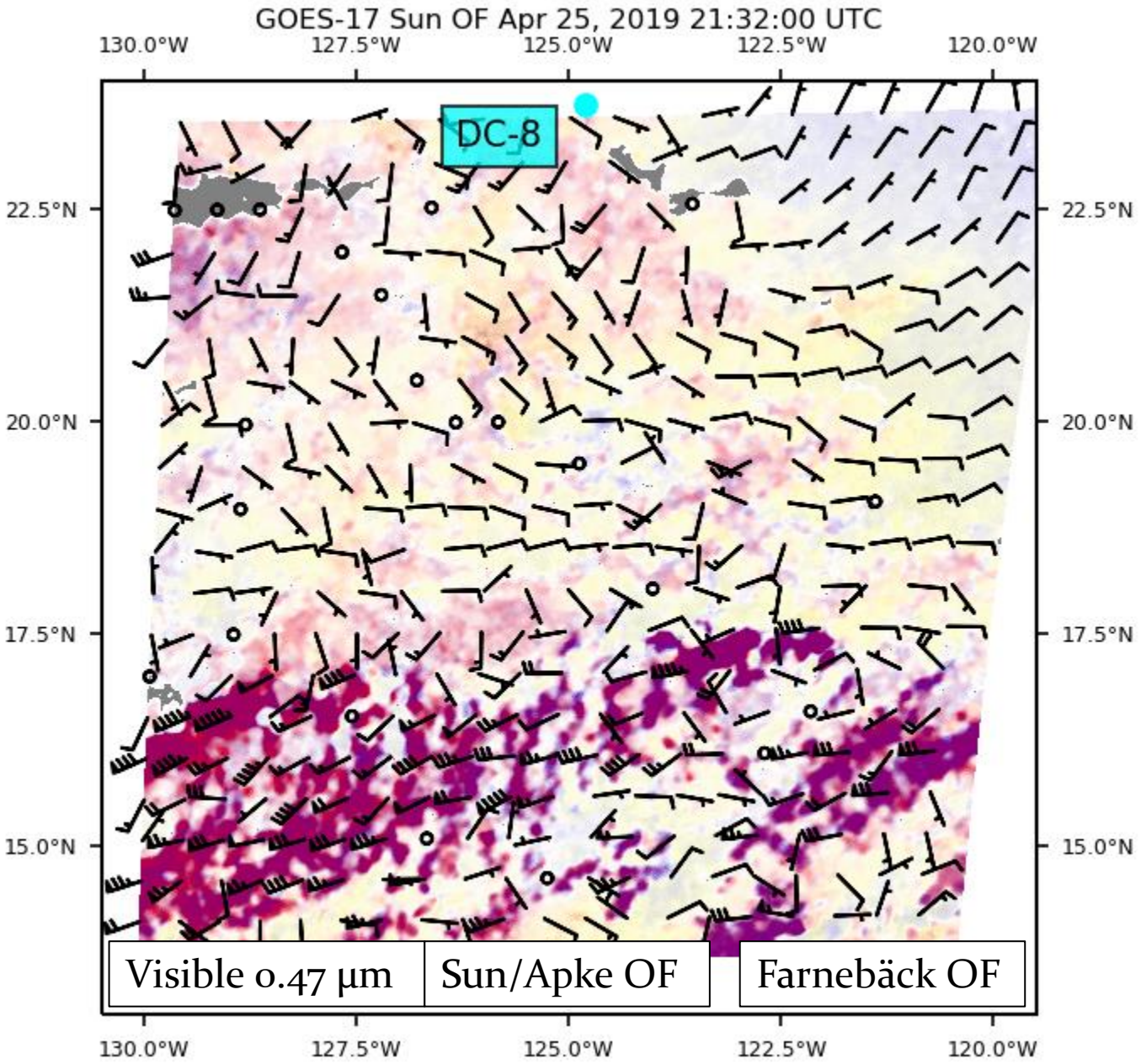

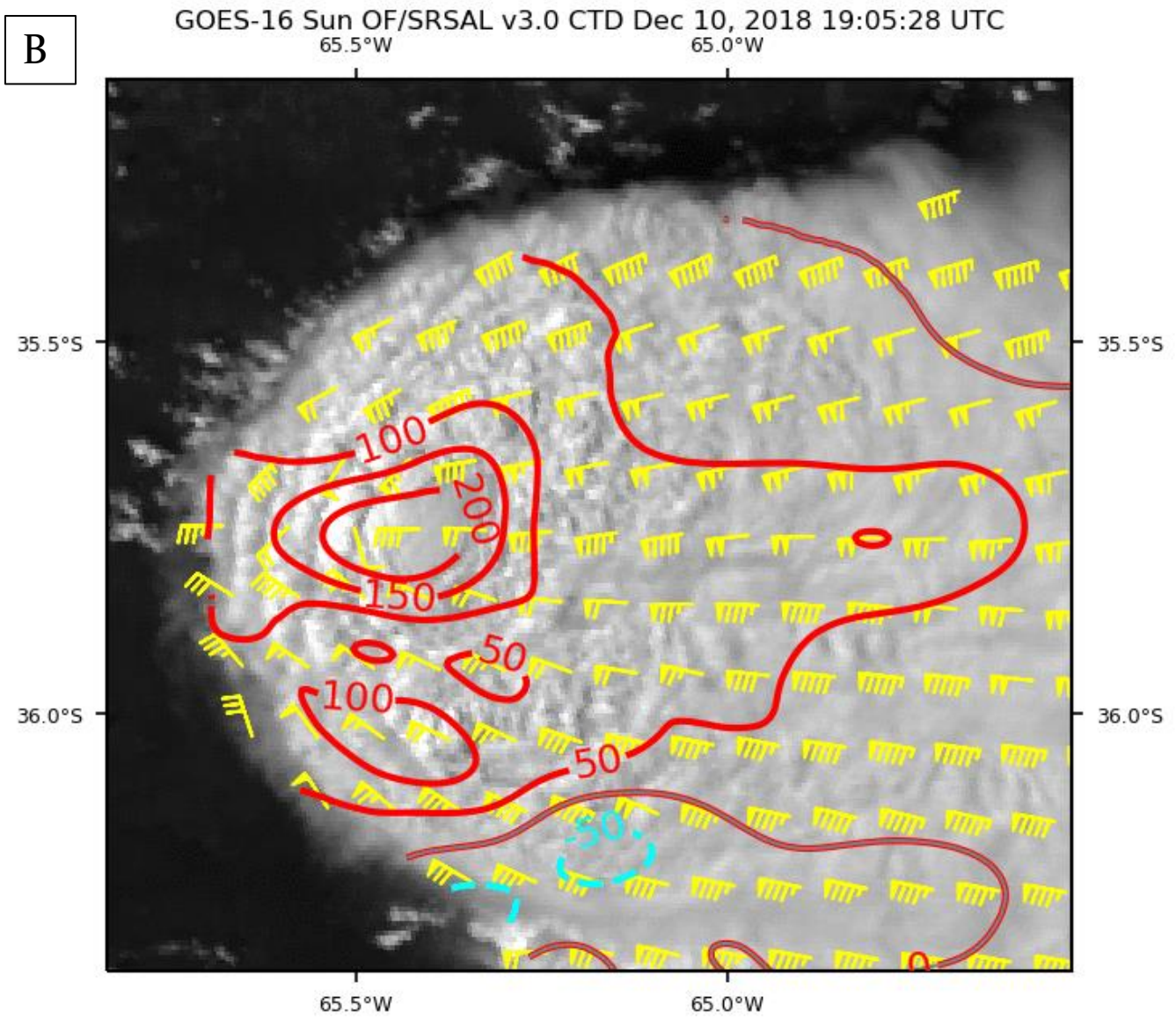

- Derived from dense optical flow, deep convection cloud-top divergence highlights the most intense updrafts in image loops
- From a large sample of updrafts, overshooting tops with higher CTD were more likely to be associated with deep, severe weather producing convection

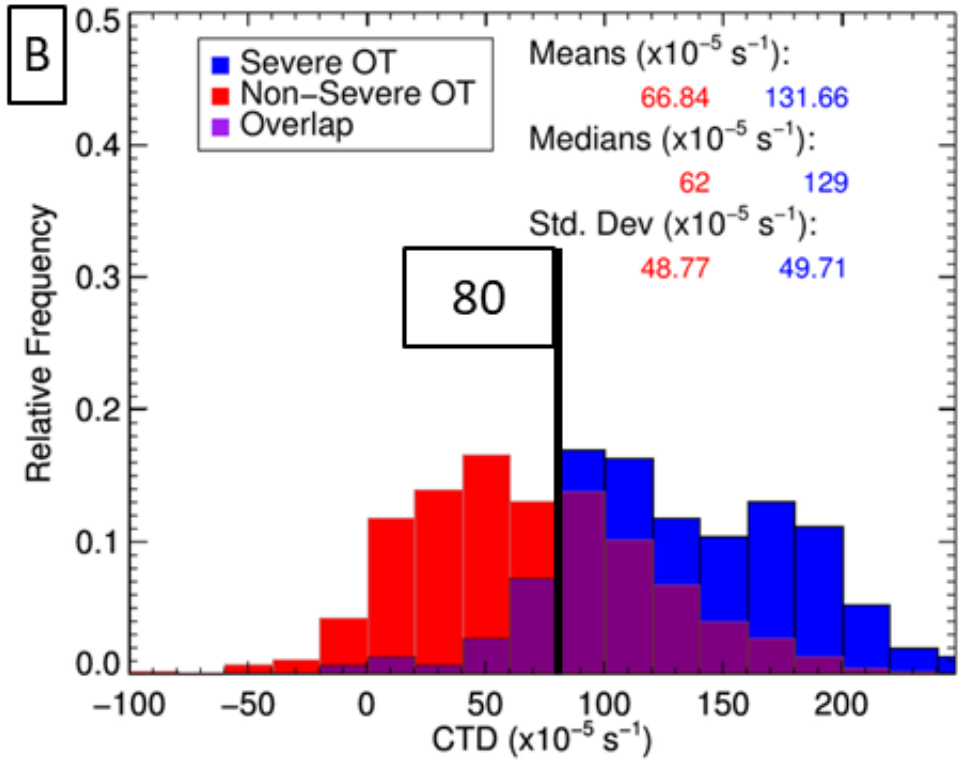

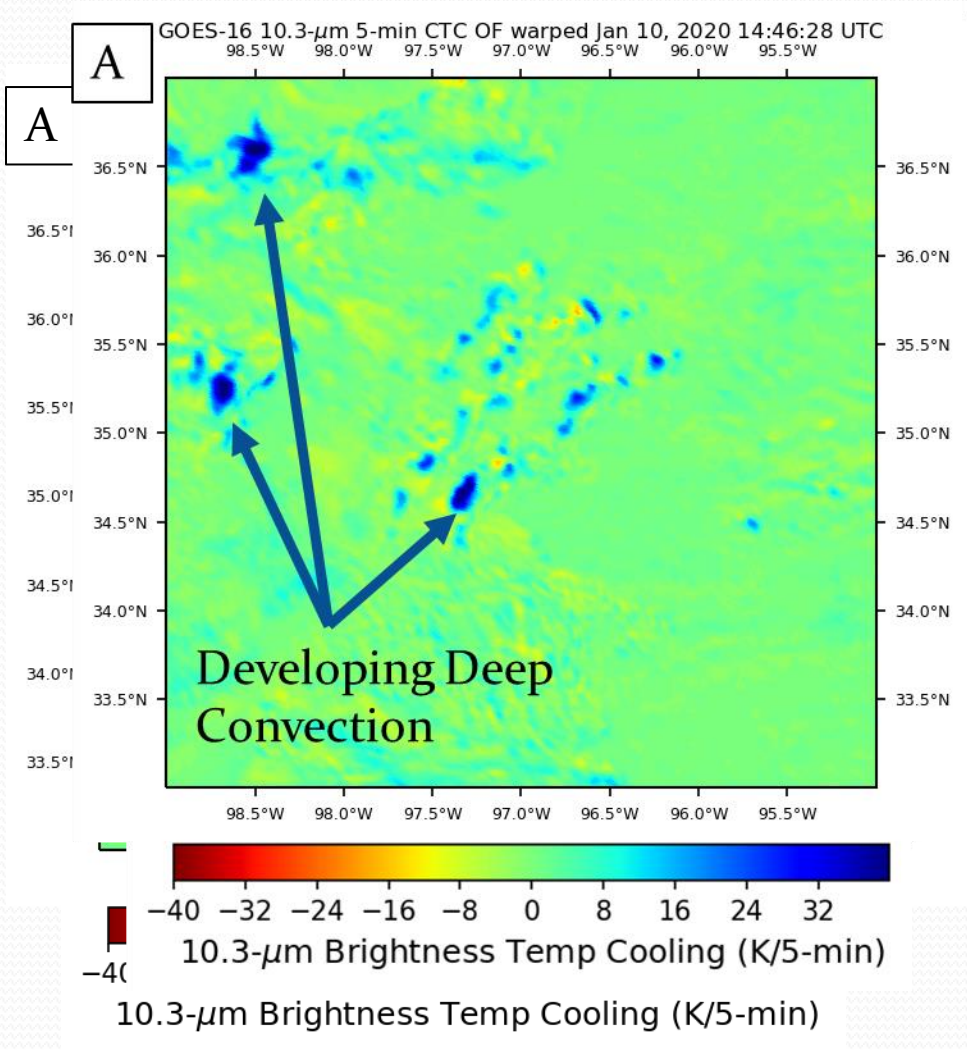
A
GOES-16 10.3-μm 5-min CTC OF warped Jan 10, 2020 14:46:28 UTC
98.5°W 98.0°W 97.5°W 97.0°W 96.5°W 96.0°W 95.5°W
36.5°N
36.0°N
35.5°N
35.0°N
34.5°N
34.0°N
33.5°N
Developing Deep Convection
−40 −32 −24 −16 −8 0 8 16 24 32
10.3-μm Brightness Temp Cooling (K/5-min)

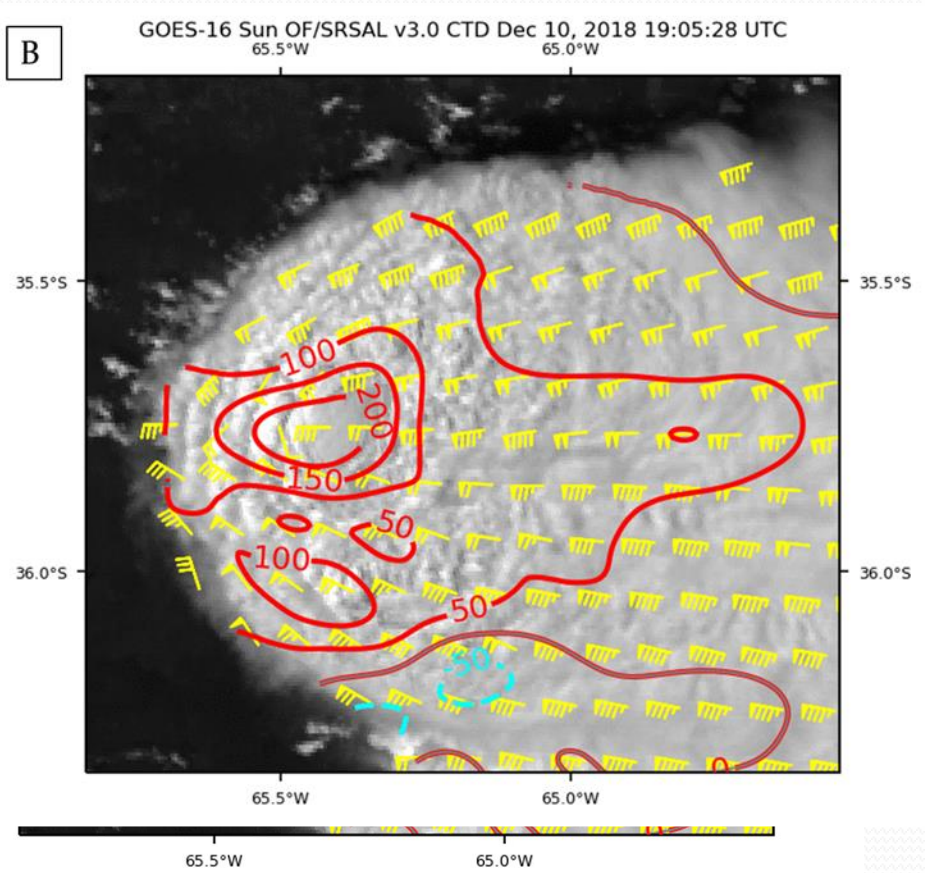
B
GOES-16 Sun OF/SRSAL v3.0 CTD Dec 10, 2018 19:05:28 UTC
65.5°W
65.0°W
35.5°S
36.0°S
100
200
150
50
100
50
-50
0
65.5°W
65.0°W